



European Reviews of Chemical Research

Has been issued since 2014.
E-ISSN 2413-7243
2020. 7(1). Issued once a year

EDITORIAL BOARD

Bekhterev Viktor – Sochi State University, Sochi, Russian Federation (Editor in Chief)
Belskaya Nataliya – Ural Federal University, Ekaterinburg, Russian Federation
Kuvshinov Gennadiy – Sochi State University, Sochi, Russian Federation
Elyukhin Vyacheslav – Center of Investigations and Advanced Education, Mexico, Mexico
Kestutis Baltakys – Kaunas University of Technology, Kaunas, Lithuania
Mamardashvili Nugzar – G.A. Krestov Institute of Solution Chemistry of the Russian Academy of Sciences, Ivanovo, Russian Federation
Maskaeva Larisa – Ural Federal University, Ekaterinburg, Russian Federation
Md Azree Othuman Mydin – Universiti Sains Malaysia, Penang, Malaysia
Navrotskii Aleksandr – Volgograd State Technical University, Volgograd, Russian Federation
Ojovan Michael – Imperial College London, London, UK

Journal is indexed by: **CrossRef** (UK), **Electronic scientific library** (Russia), **Journal Index** (USA), **Open Academic Journals Index** (USA), **ResearchBib** (Japan), **Scientific Indexing Services** (USA)

All manuscripts are peer reviewed by experts in the respective field. Authors of the manuscripts bear responsibility for their content, credibility and reliability.

Editorial board doesn't expect the manuscripts' authors to always agree with its opinion

Postal Address: 1367/4, Stara Vajnorska str., Bratislava – Nove Mesto, Slovakia, 831 04
Release date 15.12.20
Format 21 × 29,7/4.

Website: <http://ejournal14.com/en/index.html> Headset Georgia.
E-mail: aphr.sro@gmail.com

Founder and Editor: Academic Publishing House Researcher s.r.o. Order № 115.

European Reviews of Chemical Research

2020

Is. **1**

CONTENTS

Articles

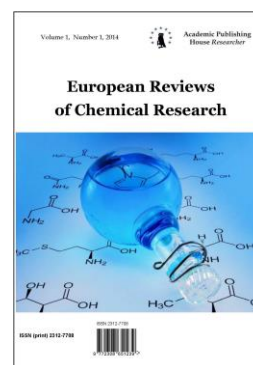
Molecular Docking Study of Primaquine-Favipiravir Based Compounds as Potential Inhibitors of COVID-19 Main Protease O.F. Akinyele, E.G. Fakola, O.E. Oyeneyin, O.O. Adeboye, A.O. Ayeni, J.S. Amoko, T.A. Ajayeoba	3
Biochemical Effects of Aqueous Leaf Extract of Abeere (Hunteria Umbellata) on Liver Enzymes of Albino Rats I.A.A. Ibrahim, L.A. Magashi	16
Solvatochromic and Halochromic Evaluation of Some Biheterocyclic Cyanine Dyes H.A. Shindy, M.A. El-Maghraby, F.M. Eissa	20

Copyright © 2020 by Academic Publishing House Researcher s.r.o.



Published in the Slovak Republic
European Reviews of Chemical Research
Has been issued since 2014.
E-ISSN: 2413-7243
2020, 7(1): 3-15

DOI: 10.13187/erch.2020.1.3
www.ejournal14.com



Articles

Molecular Docking Study of Primaquine-Favipiravir Based Compounds as Potential Inhibitors of COVID-19 Main Protease

Olawale F. Akinyele^a, Emmanuel G. Fakola^a, Oluwatoba E. Oyeneyin^{b,*}, Omolara O. Adeboye^c, Ayowole O. Ayeni^a, Justinah S. Amoko^d, Temitope A. Ajayeoba^a

^aObafemi Awolowo University, Ile-Ife, Osun State, Nigeria

^bAdekunle Ajasin University, Akungba-Akoko, Ondo State, Nigeria

^cEmmanuel Alayande College of Education, Oyo, Oyo State, Nigeria

^dAdeyemi College of Education, Ondo, Ondo State, Nigeria

Abstract

The continuous search for drugs that can combat COVID-19 virus is very important in a bid to save lives and address failing economies. Schiff bases and amide compounds derived from the fusion of primaquine (a 4-aminoquinoline antimalarial) and favipiravir are hereby reported because of suitable synthetic approaches and are investigated for their potential as drug candidates against the virus. The molecular docking results using iGEMDOCK and LeDock showed that the compounds had better interaction with the protease protein of the coronavirus (6LU7) as they displayed better scores than the standard drugs used in the study (chloroquine and favipiravir). The high binding affinity could be as a result of the fusion of both drug candidates. The docking results were analyzed using Discovery Studio and PyMOL. The druglikeness showed that they qualify as oral drug candidates, hence these compounds could serve as potential inhibitors of COVID-19, subject to further clinical and pre-clinical probes.

Keywords: COVID-19 inhibitors, primaquine, favipiravir, drug-likeness, Schiff bases, amides.

1. Introduction

Coronaviruses were first reported in 1947 (Bailey et al., 1949), since then several viruses under the same family have been discovered and reported, they were first known to infect animals in a very severe manner (Pillaiyar et al., 2016). However, their recent infection on man has triggered serious interest in the understanding of these classes of viruses as well as ways to deal with them, especially as they are associated with deadly diseases from severe acute respiratory syndrome (SARS). These viruses are members of two subfamilies coronaviridae belonging to the order Nidovirales.

The discovery of a new strain of coronaviruses responsible for an outbreak in Wuhan, China alerted health related bodies to take up measures towards curtailing the outbreak. The outbreak,

* Corresponding author

E-mail addresses: emmanueltoaba90@gmail.com (O.E. Oyeneyin)

which was later considered to be one of the Public Health Emergencies of International Concern (PHEIC) by WHO, is reported to have spread to six (6) continents with more than 18.5 million infections in 188 countries and with more than 700,000 deaths (Aljazeera, 2020). It has also caused a lot of economic problems resulting from the lockdown enforced by the governments of affected countries. The organization reported that the risk assessment of the outbreak is very high and named the virus responsible for the infection of the disease. Currently, there are no established drugs or therapies for COVID-19, although WHO reports the commencement of the first vaccine trial in China. Most of the measures implemented in various countries against the infection are mainly preventive as well as supportive. In a bid to deal with the COVID-19 infection, several studies are being undertaken. Most of these studies relate to the use of existing antiviral drugs against the infection. For instance, lopinavir/ritonavir, an anti-HIV drug has been tested against the virus (Asai et al., 2020). Amidst the trials, several studies suggest that chloroquine shows potential in being effective against the virus particularly SARS-CoV (Vincent et al., 2005, Cao et al., 2020). In addition to this, it has been also reported to display considerable activity on patients infected with the COVID-19. Despite the promising potential of chloroquine, it is yet to be accepted as well as approved as an efficient drug against COVID-19.

4-Aminoquinolines have shown great potential in dealing with several infections. Members of this group like chloroquine, amodiaquine and primaquine are frontline drugs in the treatment of malaria caused by several strains of plasmodium (Deshpande, Kuppast, 2016). This is due to the presence of a common quinoline pharmacophore, which is reported to bind to heme in the parasite thus inhibiting hematin formation and causing the death of the malaria parasite. Several studies also demonstrated that 4-aminoquinoline drugs were able to interfere as well as inhibit DNA and RNA synthesis in microorganisms, inhibition of RNA synthesis is very important in dealing with viral infections. Primaquine is a quinoline based antimalarial drug which also serves as a therapy for *Pneumocystis pneumonia*. It is specifically used to prevent a relapse of malaria elicited by plasmodium vivax and ovale. It is combined with quinine or chloroquine during administration (Baird, Reickmann, 2003). It has been recommended by the WHO for use in reducing transmission in control of *P. falciparum* infection.

Favipiravir, a derivative of pyridine carboxamide is an antiviral drug that has promising prospects for combating many RNA viruses, it has displayed promising action against influenza, west Nile, flaviviruses, zika and ebola virus (Furutaa et al., 2009). Recently, it was reported to be one of the frontline medication for coronavirus disease and is presently undergoing clinical trials (Chen et al., 2020, Dong et al., 2020). Several studies concerning other viral infections suggest that it acts as a purine nucleoside or purine during viral RNA replication (Furuta et al., 2005).

Several intensive research efforts are being devoted to deal with COVID-19 pandemic, some of which include the rational design and preparations of novel drugs, and the optimization of existing drugs. This is achieved by fusing them with other drugs of known activity or compounds having units that are known to exhibit biological activity, this strategy, known as hybridization is quite attractive. The result of the fusion is a hybrid molecule with additional structural features exhibiting diverse biological roles and additional bio-activity (Sashidhara et al., 2012).

Primaquine, as mentioned earlier, is part of the family of quinoline antimalarial. The compounds in this family have a common quinoline structure and exhibit similar activities against malaria and other ailments. Although chloroquine is the most widely used among the group, other members show similar and comparable biological activity, hence most times they are combined with chloroquine to increase its activity or deal with parasitic resistance (D'Alessandro et al., 2020). Primaquine, an aminoquinoline antimalarial drug, has been reported to display similar antiviral activity like chloroquine. Several reports also reveal that it inhibits protein synthesis in virus infected cells (Kajal et al., 2013). Favipiravir, on the other hand, is promising as it is reported to show reasonable activity against the coronavirus so much that it is undergoing clinical trials.

Schiff bases refer to compounds containing $-C=N-$ (imine) functional group, they are synthesized through condensation of primary amines and carbonyl compounds. They are widely used organic compound and have applications in analytical, catalytic, and inorganic chemistry (Dhar, Taploo, 1982, Przybylski et al., 2009). In the medicinal and pharmaceutical fields, they have varied applications as they exhibit several biological activities, some of which includes antimicrobial, anticonvulsant, antitubercular activities (Aboul-Fadl et al., 2003, Chaubey, Pandeya, 2012, Ejelonu et al., 2018a, Ejelonu et al., 2018b). The nitrogen atom in Schiff bases is reported to

bond via hydrogen bond to the centre of cell constituents and impedes with normal cell processes (Boonen et al., 2012). This could lead to improved activity in the selected hybrid compounds. Amides are also very important in medicinal chemistry as many known drugs possess the amide functional group. Several important amide drugs include lidocaine, oseltamivir, sildenafil, cefotiam, paracetamol. They are known to interfere with biological processes within the cells of microorganisms.

Molecular docking is a computer-aided drug discovery/design (CADD) method used to obtain relevant information about the interaction of ligands (drugs) with biological cells via their respective receptors/proteins. Besides, it can, together with adsorption, distribution, metabolism and excretion/toxicity properties (ADME/Tox) provide relevant data that are useful for the prediction of the drug-like properties of any compound. It provides an opportunity for the identification of the most probable binding mode as well as affinity; beyond this, it gives room for better understanding of the molecular mechanism and biochemical pathways for such interaction (Chen et al., 2017, Olanrewaju et al., 2020, Metibemu et al., 2020). Therefore, this study seeks to perform molecular docking and drug-likeness on hybrid compounds; Schiff bases (PFB) and amides (PFA) obtained from the fusion of primaquine and favipiravir as drug candidates against coronavirus disease. It is expected that the hybrid candidates will display excellent bioavailability and bioactivity different from the drugs selected for this study. This is geared towards developing drug candidates that are more effective in dealing with the coronavirus. The modeled compounds are to be docked with the protease protein of the coronavirus downloaded from the protein data bank with code name 6LU7. The protease structure of this virus our target for the drug design as several antiviral drugs act by inhibiting the proteolytic maturation of viruses. Chloroquine and Favipiravir are used as standards for comparison in this study, since they are leading drug candidates for combating COVID-19.

2. Results

2.1. Chemistry

The proposed method for the synthesis of the compounds is thus:

- The favipiravir is reduced to an aldehyde, the product undergoes a condensation reaction with primaquine to form Schiff bases (Figure 1).
- Favipiravir is hydrolyzed to a carboxylic acid, which reacts with primaquine to form an amide via condensation (Figure 2).

Schiff bases

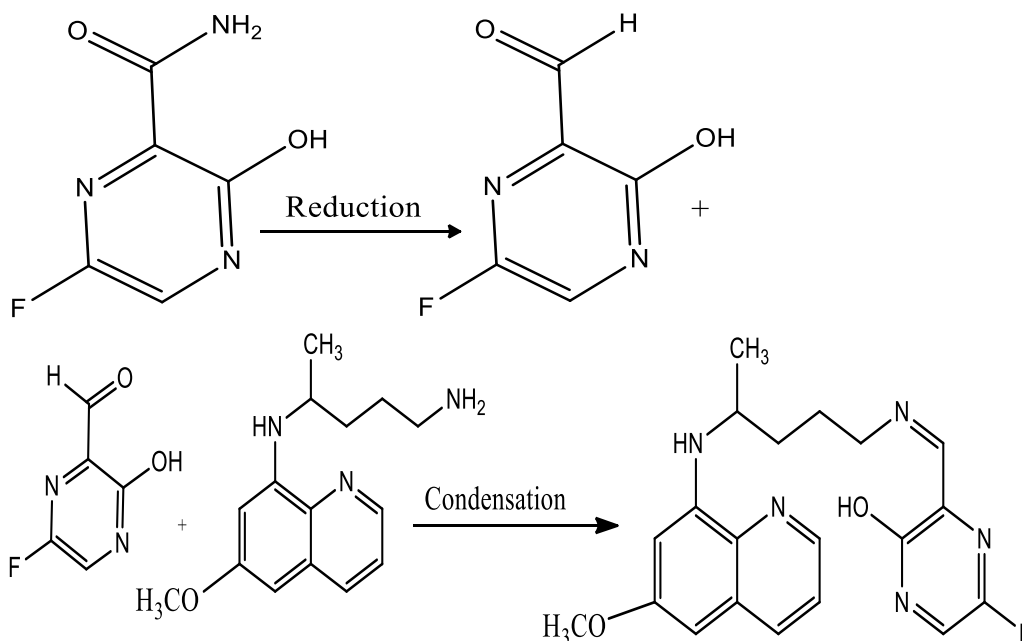


Fig. 1. Synthetic route for the Schiff bases

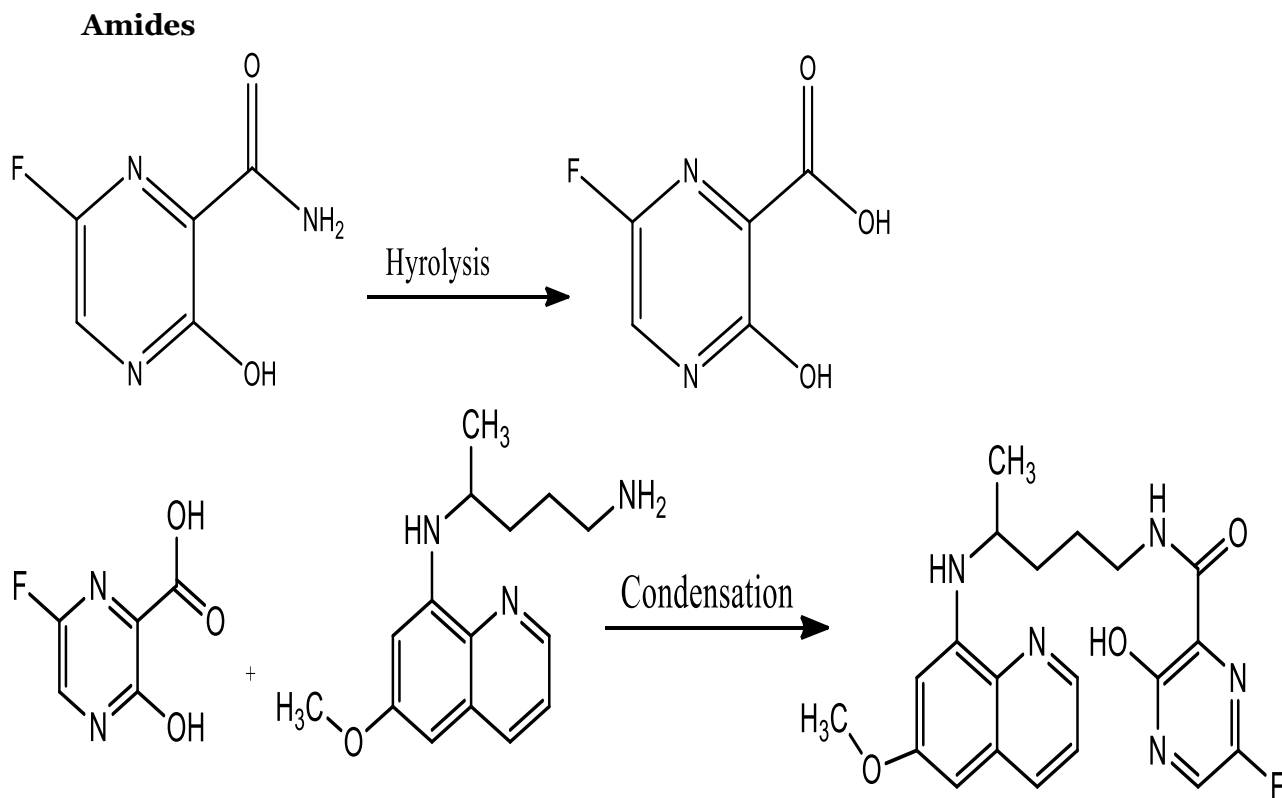
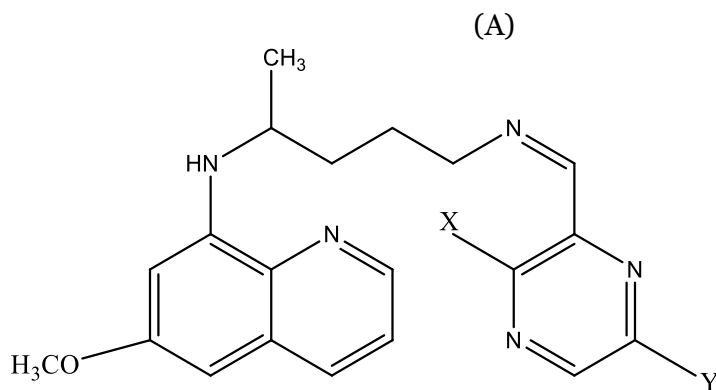


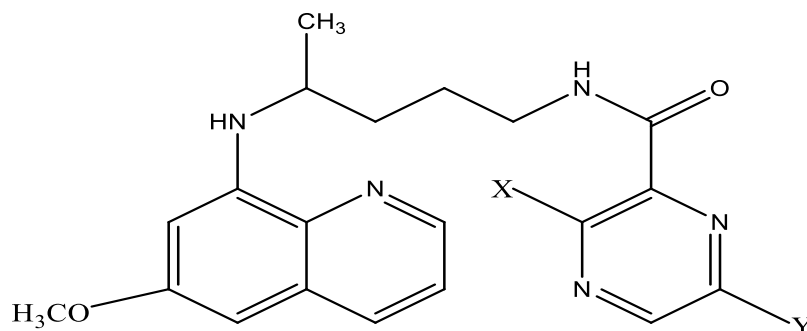
Fig. 2. Proposed method for the synthesis of amide compounds

Certain structural changes were made to both the Schiff bases and amides shown in [Figure 1](#) and [Figure 2](#) by changing the substituents to produce different compounds with the same basic pharmacophore. This is an effort to study the effect of the substituents on the pharmacophore of the hybrid compounds. The structures of the compounds employed in this study are shown ([Figure 3](#)).



(Z)-N¹-((6-fluoro-3-methylpyrazin-2-yl)methylene)-N⁴-(6-methoxyquinolin-8-yl)pentane-1,4-diamine derivatives

(B)



6-fluoro-3-hydroxy-*N*-(4-((6-methoxyquinolin-8-yl)amino)pentyl)pyrazine-2-carboxamide derivatives
 X = OH, H and Y = F, Cl

Fig. 3. Structures of Primaquine-Favipiravir Schiff bases and Amides

- (A) Schiff bases PF1B, PF2B, PF3B and PF4B
 (B) Amides PF5A, PF6A, PF7A and PF8A

2.2. Molecular docking

The crystal structure of the COVID-19 main protease (6LU7) was retrieved from the protein data bank (www.rcsb.org). The protease 6LU7 (resolution 2.16 Å) is a homodimer comprising two chains A and C with co-crystallized ligand, *n*-[(5-methylisoxazol-3-yl) carbonyl]alanyl-*l*-valyl-*n*-1-~((1*r*,2*z*)-4-(benzyloxy)-4-oxo-1-[(3*r*)-2-oxopyrrolidin-3-yl]methyl}but-2-enyl)-*l* leucinamide. The structure of the compounds was prepared in .mol2 format using Chem 3D Pro and was optimized with MMFF94 Force Field using Avogadro 1.2.9 (Hanwell et al., 2014). These optimized compounds were docked with 6LU7 using two docking softwares for comparison: namely iGEMDOCK (Hsu et al., 2011) and LeDock (Zhao, 2017).

iGEMDOCK is a protein-ligand software which employs the application of a sophisticated biologically driven computational technique. It predicts the binding to the protein target of different molecules as well as evaluating the scoring function from the generated poses. The application of iGEMDOCK to several protein systems has shown that it has an accuracy that is comparable to other docking softwares. LeDock is a docking software that relies on the amalgamation of simulated annealing and evolutionary optimization of the position of the ligand, orientation as well as the rotatable bonds utilizing a scoring scheme based on the knowledge of physics which originated from prospective virtual screening campaigns (Zhao, Huang, 2011). The results were visualized using Discovery Studio 4.5 (BIOvIA, 2015) and PyMOL version 1.7.5.0 in order to understand the protein-ligand interactions. The docking procedure included the followings: binding site preparation, ligand preparation, setting up the receptor's binding site, dock ligands, analysis of results in terms of fitness and score. The results are shown in (Table 1) below.

For iGEMDOCK, the fitness score in the binding site is given as the total energy of a predicted pose. This fitness score is the empirical scoring function given by the following expression (eq. 1),

$$F = v + H + E \dots \dots \dots 1$$

F is Fitness score, *v*, represents van der Waals energy, H, is hydrogen bonding while, Elec. represents the electrostatic energy.

2.3. Drug-likeness

The ADME (Absorption, Distribution, Metabolism, Excretion) and toxicity properties of the compounds were predicted using SWISS ADME (<http://www.swissadme.ch/>) (Daina et al., 2016). The drug-like properties were evaluated on the basis of Lipinski's rule. Druglikeness is an essential concept in drug discovery and delivery. It deals with how drug like a substance is with respect to a lot of factors. A drug like molecule is expected to show certain kind of characteristics with respect to solubility, lipophilicity, bioavailability, molecular structure etc. The Lipinski's rule of five is a standard for assessing druglikeness, however, there are other criteria according to the Lipinski's rule and ADME parameters; molecules that could serve as good oral drug candidates must respect certain conditions which include: maximum five and ten, hydrogen bond donors and hydrogen

acceptors respectively, maximum molecular coefficient (MLog P) value less than 4.15, molecular mass less than 500 Daltons (Adejoro et al., 2017).

2.4. Docking

The docking scores of the compounds obtained from iGEMDOCK (Figure 4) and LeDock (Figure 5) when PF1B, PF2B, PF3B, PF4B (Schiff bases), PF5A, PF6A, PF7A and PF8A (Amides) were docked against 6LU7 are shown in Table 1.

Table 1. Molecular docking scores of the compounds against 6LU7

Compounds	Fitness score (IGEMDOCK)	Ranking	LeDock Score (ΔG)	Ranking
PF1B	-93.90	7	-6.91	7
PF2B	-87.28	8	-6.86	8
PF3B	-99.77	3	-7.43	4
PF4B	-100.48	2	-7.33	6
PF5A	-101.42	1	-7.83	2
PF6A	-94.38	6	-7.94	1
PF7A	-96.46	4	-7.46	3
PF8A	-94.70	5	-7.36	5
chloroquine	-79.77		-5.23	
Favipiravir	-60.03		-5.63	
Co-crystallized ligand	-95.57		-5.38	

The hybrid compounds (Schiff bases and amides) had better docking scores than the chosen standards i.e. chloroquine and favipiravir. The high binding affinity may be as a result of the fusion of both drug candidates. The order of the compounds with respect to their docking scores suggests that the amide based compounds (PF5A, PF6A, PF7A, PF8A) are better potential inhibitors than the Schiff bases PF1B, PF2B, PF3B, PF4B. This might be due to the presence of the carbonyl group as it is known to account for increased interaction in biomolecules via hydrogen bonding. The compounds containing the hydroxyl and fluorine groups also had better docking scores than the others. This is due to enhanced interaction between the protein and the ligand especially with respect to hydrogen bonding. The trend for the docking scores with respect to LeDock is: PF6A > PF5A > PF7A > PF3B > PF8A > PF4B > PF1B > PF2B. The fitness scores result from IGEMDOCK showed a similar trend: PF5A > PF4B > PF3B > PF7A > PF8A > PF6A > PF1B > PF2B. All the compounds had better docking scores in comparison with the standards chloroquine and favipiravir. Figures 4 and 5, show the graphical display of the docking scores between 6LU7 and PF compounds using IGEMDOCK and LeDock respectively (The binding energy is shown in minus kcal/mol, while the fitness scores is negative).

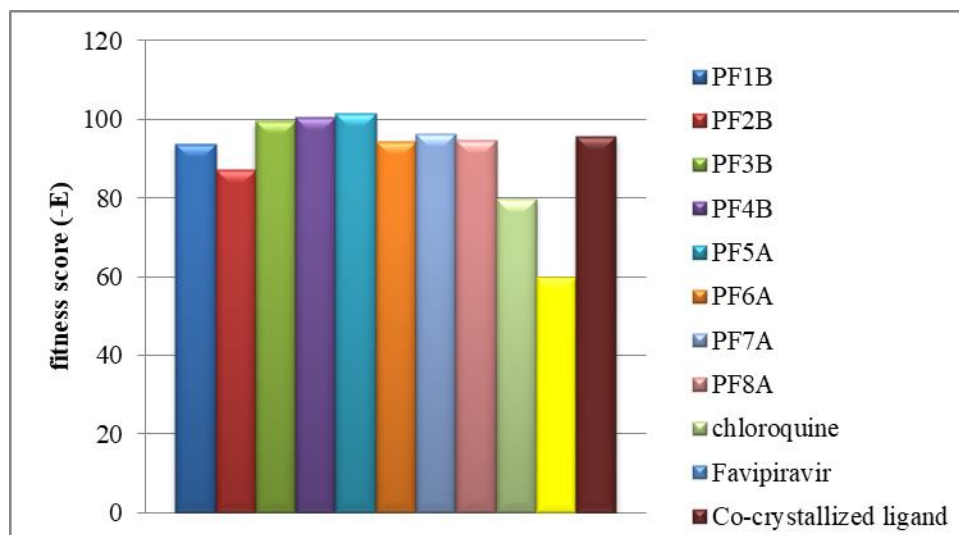


Fig. 4. Molecular docking results between 6LU7 and primaquine-favipiravir compounds using iGEMDOCK

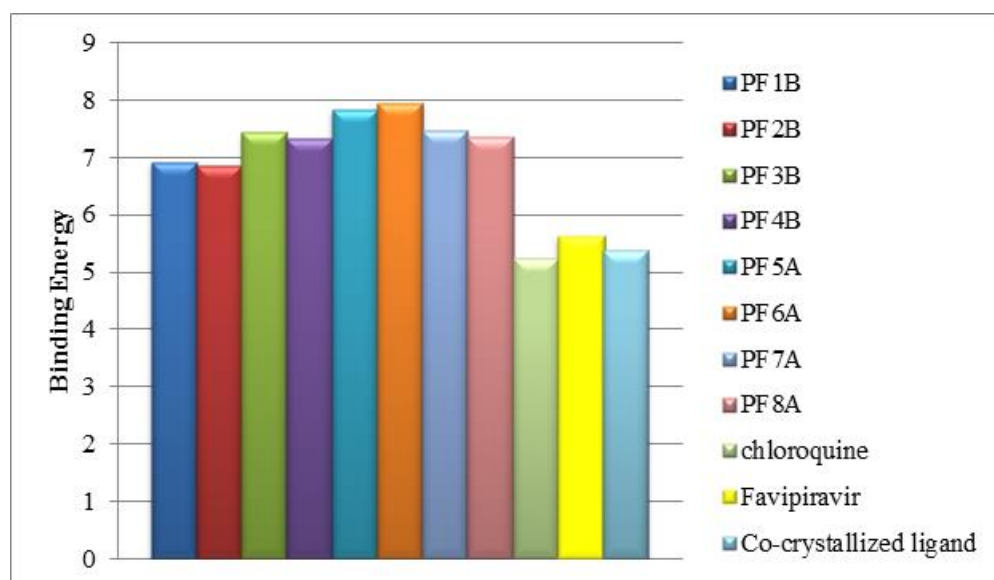


Fig. 5. Molecular docking results between 6LU7 and primaquine-favipiravir compounds using LeDock

The protein structure of 6LU7 and its co-crystallized ligand is presented (Figure 6), which reveals PHE140, LEU 141, HIS 172, HIS 164, HIS 163, LEU 167, GLY 143, HIS 41, MET 49, GLN 189, THR 190, PRO 168, ALA 191, LEU 167, GLU 166, GLU 164, HIS 164, MET 165, GLY 143 as common amino acids that interacts with the co-crystallized ligand. The mode of binding of these compounds to the target protein are shown (Figure 7a-j). The compounds interact with similar amino acids contained in the A strand of the protease protein 6LU7. Favipiravir and chloroquine both promising drugs for the treatment of the coronavirus disease interacted with PRO 168 and GLU 166. PF1B interacts with LEU 167 via an amide pi-stacked interaction and with GLU 166 and MET 165 through a carbon-hydrogen bond, it also interacts with PRO 168 via a pi-alkyl mode. PF2B and PF5A interact with just two of the amino acid; PRO 168 and ALA 191 through pi-alkyl interactions and pi-sigma bond. Others are through van der Waals interaction. PF6A interacted with PRO 168, THR 190, ALA 191, LEU 167 through pi-alkyl and amide-pi stacked interactions. PF3B and PF4B showed hydrogen bonds with ALA 191, GLY 170 the other interactions were with PRO 168 and GLU 166 via Halogen and carbon-hydrogen bond respectively. PF7A interacts with GLY 170, PRO 168, and GLU 166 via the halogen (Fluorine) other amino acids like THR 190 and

ALA 191 interacted with ligand in other ways. PF8A interacted with the protein via several amino acids namely PRO 168 through a pi-lone pair, 168, ALA 191, GLU 166 through a hydrogen bond. All these interactions account for the docking scores predicted for each ligand as the affinity of drug compounds to proteins is dependent on the type and amount of bonding that exists between the drug and protein target. The 2D diagram showing interaction between the compounds and the protein (6LU7) is shown (Figure 7). PyMOL was used to visualize the compounds in the cavity of the protein (Figure 8).

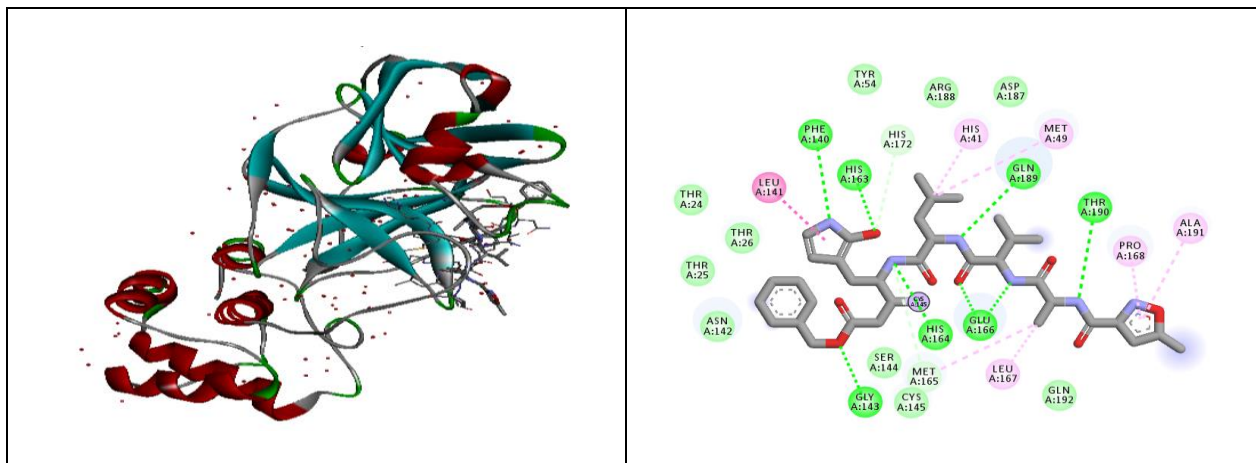
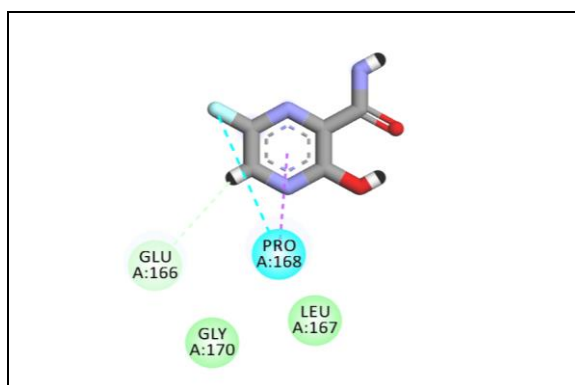
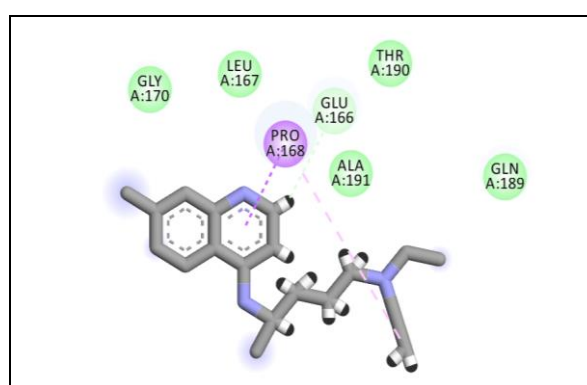


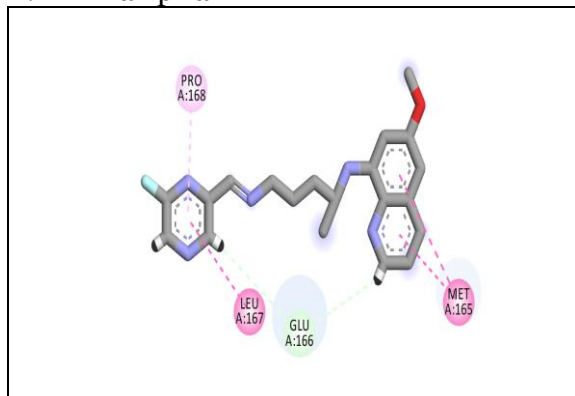
Fig. 6. The protein 6LU7 and its co-crystallized ligand



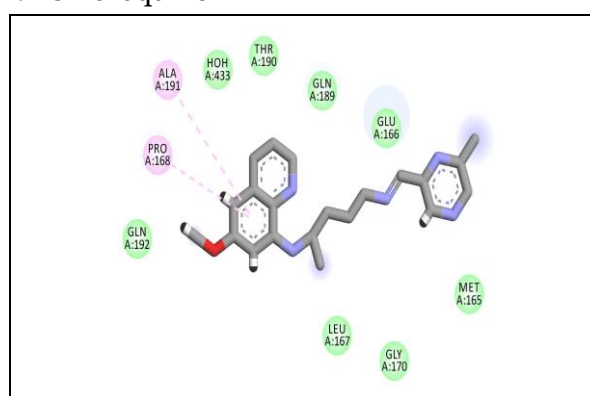
A. Favipiravir



B. Chloroquine



C. PF1B



D. PF2B

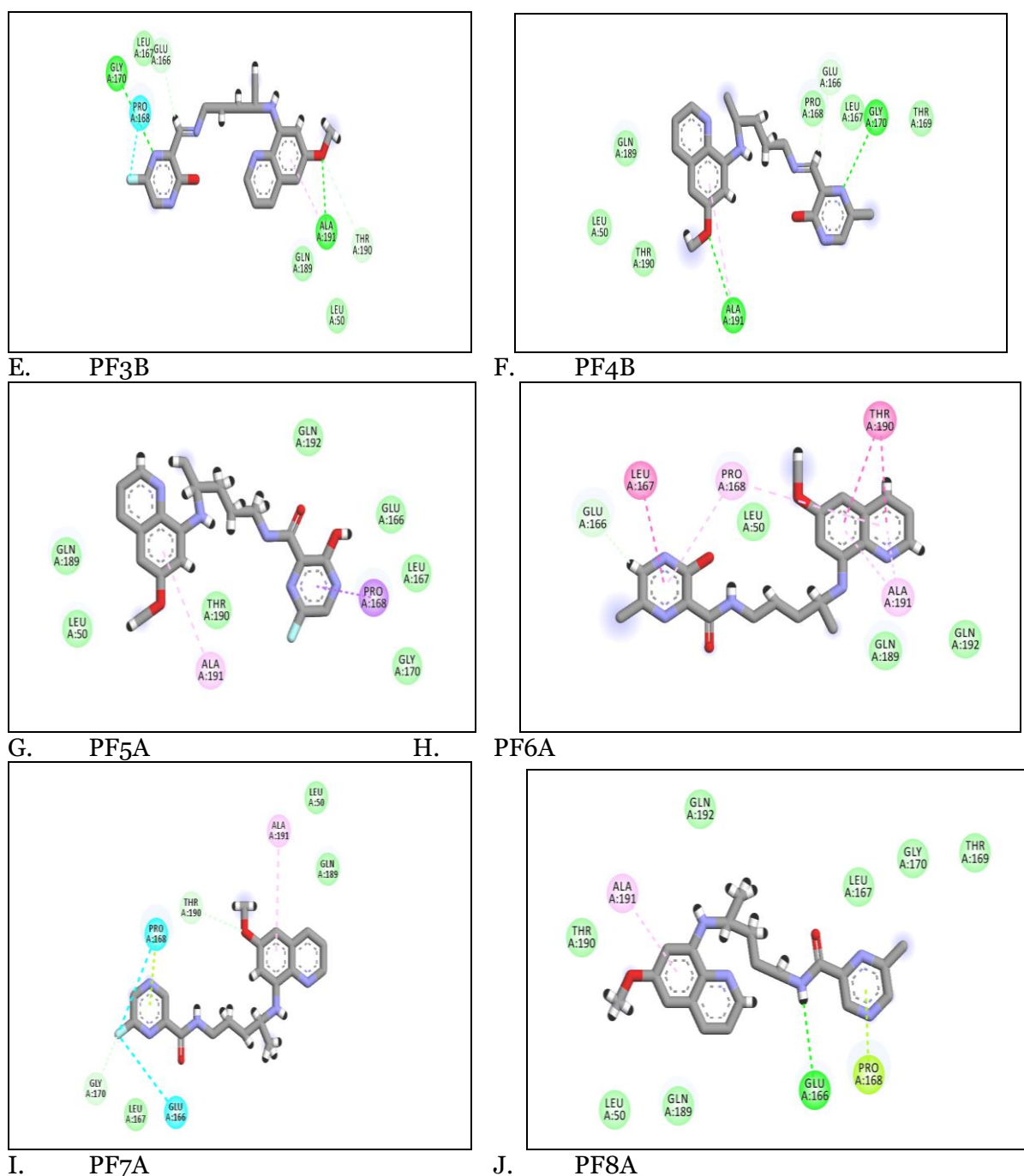


Fig. 7. 2D Diagram showing Interaction between virus main protease (6LU7), chloroquine, favipiravir and the potential inhibitor candidates

- (A) Chloroquine
- (B) Favipiravir
- (C) (Z)-5-fluoro-3-(((4-((6-methoxyquinolin-8-yl)amino)pentyl)imino)methyl)pyrazin-2-ol Schiff bases derivatives (PF1B, PF2B, PF3B and PF4B)
- (D) 6-fluoro-3-hydroxy-N-(4-((6-methoxyquinolin-8-yl)amino)pentyl)pyrazine-2-carboxamide derivatives (PF5A, PF6A, PF7A and PF8A)

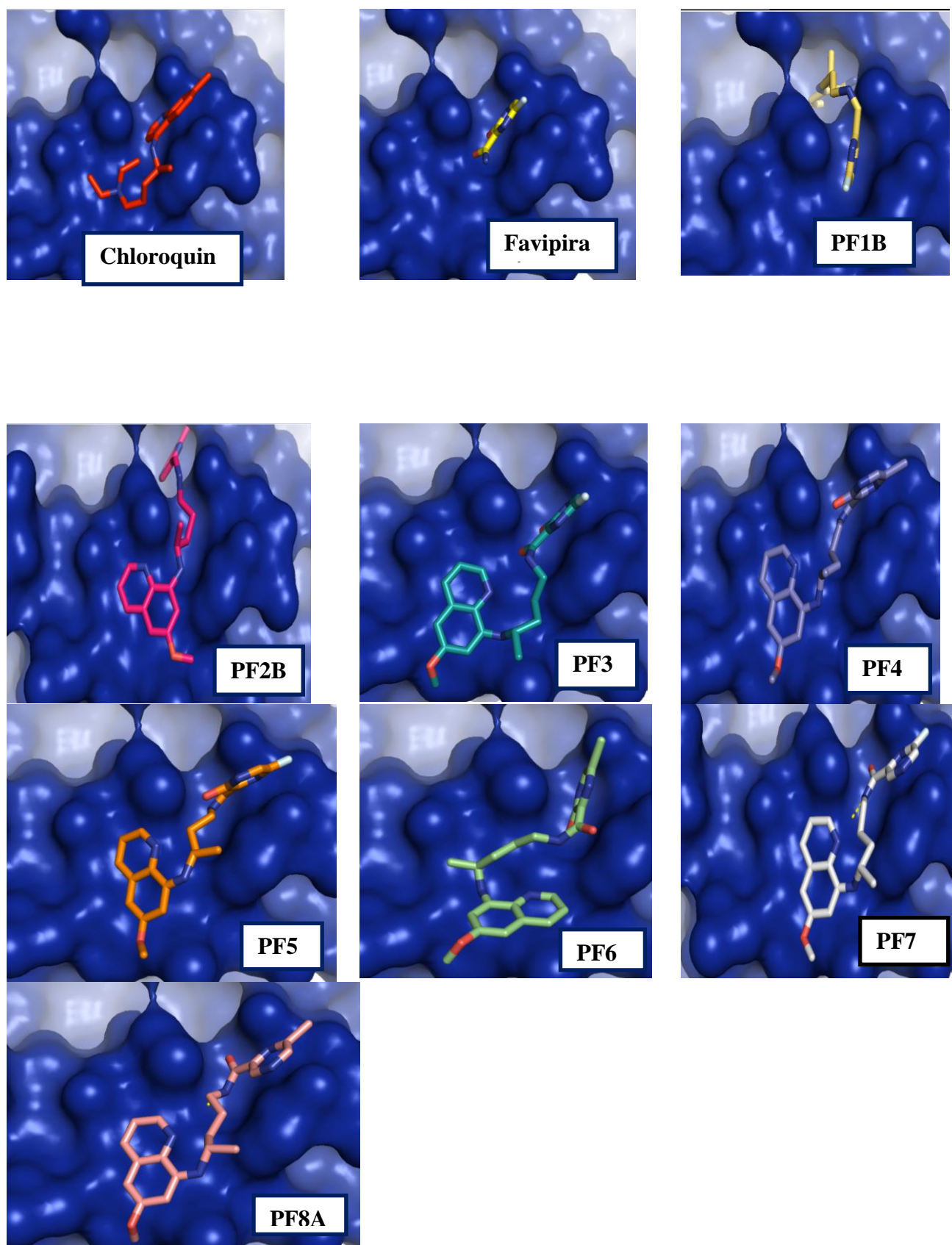


Fig. 8. Molecular docking visualization of chloroquine, favipiravir, PF1B, PF2B, PF3B, PF4B, PF5A, PF6A, PF7A and PF8A in 6LU7 using PyMOL

2.5. Druglikeness

The ADME results obtained revealed that all the compounds analyzed (PFB and PFA) qualify as drug candidates as they satisfy the conditions for oral drug candidates (Table 2).

Table 2. Druglikeness parameters for Schiff bases (PFB) and Amides (PFA)

Compounds	Formula	MW	H-bond acceptors	H-bond donors	MLOGP	Lipinski violations
PF1B	C ₂₀ H ₂₂ FN ₅ O	383.42	7	2	0.88	0
PF2B	C ₂₀ H ₂₂ ClN ₅ O ₂	399.87	6	2	0.99	0
PF3B	C ₂₀ H ₂₂ FN ₅ O	367.42	6	1	1.01	0
PF4B	C ₂₀ H ₂₂ ClN ₅ O	383.87	5	1	1.12	0
PF5A	C ₂₀ H ₂₂ ClN ₅ O ₃	399.42	7	3	0.77	0
PF6A	C ₂₀ H ₂₂ ClN ₅ O ₃	415.87	6	3	0.88	0
PF7A	C ₂₀ H ₂₂ FN ₅ O ₂	383.42	6	2	0.88	0
PF8A	C ₂₀ H ₂₂ ClN ₅ O ₂	399.87	5	2	0.99	0
Chloroquine	C ₁₈ H ₂₆ ClN ₃	319.87	2	1	3.20	0
Favipiravir	C ₅ H ₄ FN ₃ O ₂	157.10	5	2	-1.36	0

3. Conclusion

The theoretical evaluation of the Schiff bases and amides obtained from the fusion of primaquine and favipiravir exhibited better interaction with the protease derived from the coronavirus. They also gave better docking scores than the frontline drugs in the treatment of coronavirus disease, i.e. chloroquine and Favipiravir. The druglikeness studies of the proposed compounds also showed that they all qualify as potential oral drugs as they satisfy the Lipinski's rule. Thus, they could qualify as potential drug for the treatment of COVID-19, subject to confirmatory procedures for pre-clinical and clinical investigations.

4. Conflict of interest

We wish to confirm that there are no conflicts of interest associated with this publication, has not been published before and not currently being considered for publication elsewhere.

References

Aboul-Fadl et al., 2003 – Aboul-Fadl, T., Mohammed, F.A., Hassan, E.A. (2003). Synthesis, antitubercular activity and pharmacokinetic studies of some schiff bases derived from 1- alkyllisatin and isonicotinic acid hydrazide (inh). *Archives of Pharmacal Research*. 26: 778-784.

Adejoro et al., 2017 – Adejoro, I.A., Waheed, S.O., Adeboye, O.O., Akhigbe, F.U. (2017). Molecular Docking of the Inhibitory Activities of Triterpenoids of Lonchocarpus cyanescens against Ulcer. *Journal of Biophysical Chemistry*. 8(1): 1-11.

Aljazeera 2020 – Coronavirus: Which countries have confirmed cases? [Electronic resource]. URL: <https://www.aljazeera.com/news/2020/01/countries-confirmed-cases-coronavirus-200125070959786.html>

Asai et al., 2020 – Asai, A., Konno, M., Ozaki, M., Otsuka, C., Vecchione, A., Arai, T., Kitagawa, T., Ofusa, K., Yabumoto, M., Hirotsu, T., Taniguchi, M., Eguchi, H., Doki, Y., Ishii, H. (2020). COVID-19 Drug Discovery Using Intensive Approaches. *International Journal of Molecular Sciences*. 21(8): 1-9.

Bailey et al., 1949 – Bailey, O.T., Pappenheimer, A.M., Cheever, F.S., Daniels, J.B. (1949). A murine Virus (JHM) Causing Disseminated Encephalomyelitis with Extensive Destruction of Myelin. *Journal of Experimental Medicine*. 90(3): 195-212.

Baird, Reickmann, 2003 – Baird, J.K., Reickmann, K.H. (2003). Can primaquine therapy for vivax malaria be improved? *Trends in Parasitology*. 19(3): 115-120.

BIOvIA, 2015 – BIOvIA, D.S. (2015). Discovery studio modeling environment. San Diego, Dassault Systemes, Release, 4.

Boonen et al., 2012 – Boonen, J., Bronselaer, A., Nielandt, J., Veryser, L., Tre, G.D. Spiegeleer, B. (2012). Alkamid database: Chemistry, occurrence and functionality of plant N-alkylamides. *Journal of Ethnopharmacology*. 142(3): 563-590.

Cao et al., 2020 – Cao, B., Wang, Y., Wen, D., Liu, W., Wang, J., Fan, G., Ruan, L., Song, B., Cai, Y., Wei, M., Li, X., Xia, J., Chen, N., Xiang, J., Yu, T., Bai, T., Xie, X., Zhang, L., Li, C., Yuan, Y., Chen, H., Li, H., Huang, H., Tu, S., Gong, F., Liu, Y., Wei, Y., Dong, C., Zhou, F., Gu, X., Xu, J., Liu, Z., Zhang, Y., Li, H., Shang, L., Wang, K., Li, K., Zhou, X., Dong, X., Qu, Z., Lu, S., Hu, X., Ruan, S., Luo, S., Wu, J., Peng, L., Cheng, F., Pan, L., Zou, J., Jia, C., Wang, J., Liu, X., Wang, S., Wu, X., Ge, Q., He, J., Zhan, H., Qiu, F., Guo, L., Huang, C., Jaki, T., Hayden, F.G., Horby, P.W., Zhang, D., Wang C. (2020). A Trial of Lopinavir–Ritonavir in Adults Hospitalized with Severe Covid-19. *The New England Journal of Medicine*. 382(19): 1787-1799.

Chaubey, Pandeya, 2012 – Chaubey, A.K., Pandeya S.N. (2012). Synthesis and Anticonvulsant Activity (Chemo Shock) of Schiff and Mannich bases of Isatin derivatives with 2-Amino pyridine (Mechanism of Action). *International Journal of PharmTech Research*. 4(2): 590-598.

Chen et al., 2017 – Chen, F., Wang, Z., Wang, C., Xu, Q., Liang, J., Xu, X., Yang, J., Wang, C., Jiang, T., Yu, R. (2017). Application of Reverse Docking for Target Prediction of Marine Compounds with Anti-tumor Activity. *Journal of Molecular Graphics and Modelling*. 77: 372-377.

Chen et al., 2020 – Chen, C., Zhang, Y., Huang, J., Yin, P., Cheng, Z., Wu, J., Chen, S., Zhang, Y., Chen B., Lu, M., Luo, Y., Ju, L., Zhang, J., Wang, X. (2020). Favipiravir versus Arbidol for COVID-19: A Randomized Clinical Trial. *Europe PMC*.

D'Alessandro et al., 2020 – D'Alessandro, S., Scaccabarozzi, D., Signorini, L., Perego, F., Ilboudo, D.P., Ferrante, P., Delbue, S. (2020). The Use of Antimalarial Drugs against Viral Infection. *Microorganisms*. 8(1): 1-26.

Daina et al., 2016 – Daina, A., Michielin, O., Zoete, V. (2016). SwissADME : a free web tool to evaluate pharmacokinetics, drug- likeness and medicinal chemistry friendliness of small molecules. *Nat. Publ. Gr*. 1-13.

Deshpande, Kuppast, 2016 – Deshpande, S., Kuppast, B. (2016). 4-aminoquinolines: An Overview of Antimalarial Chemotherapy. *Medicinal Chemistry*. 6(1): 1-11.

Dhar, Taploo, 1982 – Dhar, D.N., Taploo, C.L. (1982) Schiff bases and their applications. *Journal of Scientific and Industrial Research*. 41: 501-506.

Dong et al., 2020 – Dong, L., Hu, S., Gao, J. (2020). Discovering drugs to treat coronavirus disease 2019 (COVID-19). *Drug Discoveries & Therapeutics*. 14(1): 58-60.

Ejelonu et al., 2018a – Ejelonu, B.C., Oyenehin, O.E., Olagboye, S.A. Akele, O.E. (2018). Synthesis, Characterization and Antimicrobial Properties of Transition Metal Complexes of Aniline and Sulphadiazine Schiff Bases as Mixed Ligands. *Journal of Chemical and Pharmaceutical Research*. 10(5): 67-73.

Ejelonu et al., 2018b – Ejelonu, B.C., Olagboye, S.A., Oyenehin, O.E., Ebiesuwa, O.A., Bada, O.E. (2018). Synthesis, Characterization and Antimicrobial Activities of Sulfadiazine Schiff Base and Phenyl Dithiocarbamate Mixed Ligand Metal Complexes. *Open Journal of Applied Sciences*. 8(8): 346-354.

Furuta et al., 2005 – Furuta, Y., Takahashi, K., Kuno-Maekawa, M., Sangawa, H., Uehara, S., Kozaki, K., Nomura, N., Egawa, H., Shiraki, K. (2005). Mechanism of Action of T-705 against Influenza Virus. *Antimicrobial Agents and Chemotherapy*. 49(3): 981-986.

[Furutaa et al., 2009](#) – Furutaa, Y., Takahashia, K., Shirakib, K., Sakamotoc, K., Smeed, D.F., Barnardd, D.L., Gowend, B.B., Julanderd, J.G., Morrey, J.D. (2009). T-705 (favipiravir) and related compounds: Novel broad-spectrum inhibitors of RNA viral infections. *Antiviral Research*. 82(3): 95-102.

[Hanwell et al., 2014](#) – Hanwell, M.D., Curtis, D.E., Lonie, D.C., Vandermeersch, T., Zurek, E., Hutchison, G.R. (2014). Avogadro: an advanced semantic chemical editor, visualization, and analysis platform. *Journal of Chemoinformatics*. 4: 1-17.

[Hsu et al., 2011](#) – Hsu, K., Chen1, Y., Lin, S., Yang, J. (2011). iGEMDOCK: a graphical environment of enhancing GEMDOCK using pharmacological interactions and post-screening analysis. *BMC Bioinformatics*. 12(1): 1-11.

[Kajal et al., 2013](#) – Kajal, A., Bala, S., Kamboj, S., Sharma, N, Saini, V. (2013). Schiff Bases: A Versatile Pharmacophore. *Journal of Catalysts*. 1-14.

[Metibemu et al., 2020](#) – Metibemu, D.S., Oyenejin, O.E., Omotoyinbo, D.E., Adeniran, O.Y., Metibemu, A.O., Oyewale, M.B., Yakubu, O.F., Omotuyi, I.O. (2020). Molecular Docking and Quantitative Structure Activity Relationship for the Identification of Novel Phyto-inhibitors of Matrix Metalloproteinase-2. *Science Letters*. 8(2): 61-68.

[Olanrewaju et al., 2020](#) – Olanrewaju, A.A., Ibeji, C.U., Oyenejin, O.E. (2020). Biological evaluation and molecular docking of some newly synthesized 3d-series metal(II) mixed-ligand complexes of fluoro-naphthyl diketone and dithiocarbamate. *SN Applied Sciences*. 2(4): 678.

[Pillaiyar et al., 2016](#) – Pillaiyar, T., Manickam, M., Namasivayam, V., Hayashi, Y., Jung, S. (2016). An Overview of Severe Acute Respiratory Syndrome-Coronavirus (SARS-CoV) 3CL Protease Inhibitors: Peptidomimetics and Small Molecule Chemotherapy. *Journal of Medicinal Chemistry*. 59(14): 6595-6628.

[Przybylski et al., 2009](#) – Przybylski, P., Huczynski, A., Pyta, K., Brzezinski, B., Bartl, F. (2009). Biological Properties of Schiff Bases and Azo Derivatives of Phenols. *Current Organic Chemistry*. 13(2): 124-148.

[Sashidhara et al., 2012](#) – Sashidhara, K.V., Kumar, M., Modukuri, R.K. Srivastava, R.K., Soni, A., Srivastava, K., Singh, S.V., Saxena, J.K., Gauniyal, H.M., Puri, S.K. (2012). Antiplasmodial activity of novel keto-enamine chalcone-chloroquine based hybrid pharmacophores. *Bioinorganic and Medicinal Chemistry*. 20(9): 2971-2981.

[Vincent et al., 2005](#) – Vincent, M.J., Bergeron, E., Benjannet, S., Erickson, B.R., Rollin, P.E., Ksiazek, T.G., Seidah, N.G., Nichol, S.T. (2005). Chloroquine is a potent inhibitor of SARS coronavirus infection and spread. *Virology Journal*. 2(69).

[Zhao, 2017](#) – Zhao, H. (2017). User Guide for LeDock. [Electronic resource]. URL: www.lephar.com

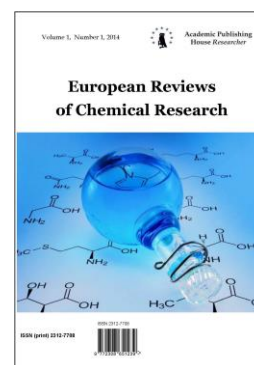
[Zhao, Huang, 2011](#) – Zhao, H., Huang, D. (2011). Hydrogen bonding penalty upon ligand binding. *Plus One*. 6(6): 1-8.

Copyright © 2020 by Academic Publishing House Researcher s.r.o.



Published in the Slovak Republic
European Reviews of Chemical Research
Has been issued since 2014.
E-ISSN: 2413-7243
2020, 7(1): 16-19

DOI: 10.13187/erch.2020.1.16
www.ejournal14.com



Biochemical Effects of Aqueous Leaf Extract of Abeere (*Hunteria Umbellata*) on Liver Enzymes of Albino Rats

Iliyasu A.A. Ibrahim ^{a,*}, Labaran A. Magashi ^b

^a Department of Science Laboratory Technology, Faculty of Science, Bauchi State University, Gadau, Bauchi, Nigeria

^b Chemistry Department, College of Education Gidan-Waya, Kafanchan, Kaduna, Nigeria

Abstract

The research was conducted to ascertain the hepatotoxic potentials of the leaves extract of *Hunteria umbellata* on liver enzymes of apparently healthy albino rats. A total of sixteen (16) albino rats were clustered into four (4) groups of four (4) rats each designated as group A – D, Group A served as control while groups B, C and D were treated with 200 mg/kg, 300 mg/kg, and 400 mg/kg aqueous leaves of extract of *Hunteria umbellata* respectively for a period of two weeks. The liver enzymes were determined using spectrophotometric methods. The results show a significant increase ($P < 0.05$) of serum AST activity at all doses. A similar trend was seen in the activity of serum ALP where a significant decrease was observed ($P < 0.05$) at all doses. There was a continuous decrease in the activity of serum ALT as the dose was increased but the increase was not significant ($P < 0.05$). The extract appears to have significant effects ($P < 0.05$) on serum AST, ALP activity but exhibited no significant effects on serum ALT and the Albumin concentration when compared with control rats. In conclusion, acute oral administration of the extracts was found to be quite toxic relatively safe at a low brought alteration in the serum AST and ALP activity but appears to have no significant effect on serum ALT activity.

Keywords: *hunteria umbellata*, hepatic, ALP, AST, ALT, liver and enzymes.

1. Introduction

Hunteria umbellata is a shrub or small tree with a dense crown; it can grow up to 10-15 metres tall with exceptional specimens to 22 metres (Ibeh et al., 2007). The bole, which is fluted and can be sinuous or straight, is 40-55 cm in diameter. The plant has a colourless or milky latex in all of its parts. The tree is valued locally for its timber and also has a range of medicinal uses. The bark is sometimes exported, mainly to Germany, for medicinal use (Oboh et al., 2019).

Hunteria umbellata grows as either a shrub or small tree up to 22 metres tall, with a trunk diameter of up to 40 centimetres. Its flowers feature a white, creamy or pale yellow corolla. The fruit is yellow and smooth. Its habitat is forests from sea level to 600 metres altitude (Oluwamodupe Cecilia Ejeloni, 2019).

Although all parts of the plant are toxic and fatalities have been recorded, the roots and bark are often used in traditional medicine in Africa (Athira, Jayaraman, 2018). A number of alkaloids have been detected in the plant (Jaca, Kambizi, 2011).

* Corresponding author

E-mail addresses: iliasuibrahim@gmail.com (I.A.A. Ibrahim)

Some 20 indole alkaloids have been isolated, most occurring in the stem bark and root bark.

The alkaloids eburnamonine, eburnamine and hunterine show cardio-vascular properties, some symphathomimetic properties and a strong and lasting hypotensive action (Adeneye Adejuwon et al., 2013).

Research supports the traditional use of seed extracts in Nigeria for the treatment of diabetes, as it increases the activity of glucokinase and lowers blood glucose levels (Nazar et al., 2016).

Aqueous and methanolic extracts of the leaves, seeds and stem bark have shown significant anthelmintic activity against earthworms (Chekole, 2017). Tests with leaf extracts have shown molluscicidal action on the freshwater snail *Bulinus globulus* (Momodu et al., 2014). The powdered root and root-decoction are used to prevent miscarriage and in the treatment of menorrhoea (Pereira et al., 2019). The root and stem bark are used as an anthelmintic, especially against guinea worm, filaria worms and schistosomiasis (causing ilharzia) (Pereira et al., 2019).

Externally, the bark is used as a lotion to treat fevers and the fresh root-bark extract is applied to sores caused by leprosy (Jima, Megersa, 2018).

Aqueous and alcoholic extracts of the seeds are used as a cure for piles, yaws, diabetes and stomach ulcers. A bark or fruit decoction is taken to treat stomach-ache, liver problems and hernia. The plant is also used in the treatment of geriatric problems. There appears to be no data on its toxicological effects, especially those on liver enzymes. The research therefore aims to study the effects of the plant on same.

2. Materials and methods

Plant Materials

The fresh leaf of *Hunteria umbellata* was purchased from Olodi Apapa market in Lagos State, Nigeria and was brought to the Biological Science Department, Abubakar Tafawa Balewa University Bauchi.

Preparation of the Extract

The leaves were sorted out separately to obtain only fresh leaves and washed with distilled water without squeezing to remove debris and dust particle. They were air-dried and ground into coarse powder using pestle and mortar and sieved to fine powder. 150 g of the fine powder was extracted or cold macerated into 900 ml of distilled water for 24 hours and the macerated mixture was then filtered through muslin cloth. It was then filtered to obtain the *Hunteria umbellata* and mixture of aqueous extract through filter paper. The filtrate was dried in an electric oven at 50°C until a semisolid residue dark solid extract was obtained.

Experimental Animals

Sixteen (16) white albino rats with weighed between 80-100 g were purchased from National Veterinary Research Institute (NVRI) Vom, Plateau State. The animals were placed in cages and fed appropriately at biological science department, Abubakar Tafawa Balewa University Bauchi.

Experimental Design

At the end of the seven days' acclimatization period, the animals were randomly assigned into four different groups of four rats each, designated as groups of A – D. Group A received water and feed only and serves as control, group B were administered orally with 200 mg/kg, group C were administered orally with 300 mg/kg and group D were administered orally with 400 mg/kg doses of the extract for the period of fourteen days. On the 15th day all the rats were sacrificed and blood sample collected.

Administration of the Extract

Administration of the extract was done via oral route with the aid of oral cannula and syringe. Animals received their doses once per day for the period of two weeks. They were observed daily for clinical signs of toxicity or pharmacological signs, throughout the period of study.

Collection of Blood

At the end of the two weeks of extract administration, the albino rats were slaughtered to obtain blood from jugular vein. The collected blood sample from each rat were allowed to clot and then centrifuged at 3000 rpm for 10 minutes. Serum was obtained used for the assay of Aspartate aminotransferase (AST), Alanine aminotransferase (ALT), and Alkaline phosphatase (ALP).

Blood Analysis

Hepatic analysis of the serum enzymes for ALT and AST was done by the method of Reitman and Frankel (1957), ALP was assayed according to the method of Rec (1972).

Estimation of Parameters

Aspartate Aminotransferase (AST) assayed using Colorimetric method of Reitman and Frankel, 1957.

Alanine Aminotransferase (ALT) assayed by Colorimetric method of Reitman and Frankel, 1957.

ALKALINE PHOSPHATASE (ALP) assayed by method of Rec, 1972.

3. Results and discussion

The results show a significant increase ($P < 0.05$) of serum AST activity at all doses. A similar trend was seen in the activity of serum ALP where a significant decrease was observed ($P < 0.05$) at all doses. There was a continuous decrease in the activity of serum ALT as the dose was increased but the increase was not significant ($P < 0.05$). The extract appears to have significant effects ($P < 0.05$) on serum AST, ALP activity but exhibited no significant effects on serum ALT and the Albumin concentration when compared with control rats.

Table 1. Effect of aqueous leaf extract of *Hunteria umbellata* on liver enzymes in normal albino rats

Grouping	Parameters Assayed		
	AST(IU/L)	ALT(IU/L)	ALP(IU/L)
Group A (Control)	5.6±0.15	2.8±0.31	106.26±8.51
Group B (200mg/kg)	7.6±0.50	2.6±0.12	92.21±1.20
Group C (300mg/kg)	8.0±0.55	2.6±0.03	78.42±1.25
Group D (400mg/kg)	8.7±0.34	2.5±0.033	66.06±0.35

Table 1 showed the effect of aqueous leaf extract of *Hunteria umbellata* on liver enzymes in normal albino rats. The activity of AST increased to 7.6±0.50 in the rats treated with 200 mg/kg body weight of the extract and increased to 8.0±0.55 and 8.7±0.34 in the rats treated with 300 and 400 mg/kg body weight of the extracts respectively when compared with untreated group (5.6±0.15) with significant ($P > 0.05$) differences. However, the activity of ALT was slightly decreased to 2.6±0.12 in the rats treated with 200mg/kg body weight of the extracts continuously decreased to 2.6±0.03 and 2.5±0.33 in the rats treated with 300 and 400 mg/kg body weight of the extracts respectively when compared with untreated group (2.8±0.31) with no significant ($P > 0.05$) difference. The result of ALP showed a significant ($P < 0.05$) decrease of serum ALP activity (92.21±1.20) was observed in the rats treated with 200 mg/kg body weight of the extracts and decreased 78.42 ±1.25 and 66.06±0.35 was observed in the rats treated with 300 and 400 mg/kg body weight of the extracts respectively when compared with untreated group (106.26±8.51).

5. Conclusion

Acute oral administration of the extracts was found to be quite toxic relatively safe at a low brought alteration in the serum AST and ALP activity but appears to have no significant effect on serum ALT activity.

6. Recommendations

Further studies should be carried out by increasing the number of experimental animals, so that larger data could be obtained so as to reach a better conclusion. Biochemical parameters associated with liver function test such as bilirubin, albumin and total protein should also be analyzed so as to find out the detail hepatotoxic effect of *Hunteria umbellata*.

Histological analysis of the liver of albino rat should also be conducted.

References

Adeneye Adejuwon et al., 2013 – Adeneye Adejuwon, A., Crooks, P.A., Fadhel-Albayati, Z., Miller, A.F., Zito, S.W., Adeyemi, O.O., Agbaje, E.O. (2013). Antihyperglycemic profile of erinidine isolated from *Hunteria umbellata* seed. *African Journal of Traditional, Complementary, and*

Alternative Medicines: AJTCAM/African Networks on Ethnomedicines.

Athira, Jayaraman, 2018 – Athira, C., Jayaraman, J. (2018). A Review on: A Pharmacological Properties of *Abelmoschus Esculentus*. *Athira et Al. World Journal of Pharmaceutical Research*. 7(12): 159-175. DOI: <https://doi.org/10.20959/wjpr201812-12211>

Chekole, 2017 – Chekole, G. (2017). Ethnobotanical study of medicinal plants used against human ailments in Gubalafto District, Northern Ethiopia. *Journal of Ethnobiology and Ethnomedicine*. DOI: <https://doi.org/10.1186/s13002-017-0182-7>

Ibeh et al., 2007 – Ibeh, I.N., Idu, M., Ejimadu, I.M. (2007). Toxicological Assessment of “Abeere” Seed *Hunteria Umbellata* K. Schum (Apocynaceae). 15(1): 4-7.

Jaca, Kambizi, 2011 – Jaca, T. P., Kambizi, L. (2011). Antibacterial properties of some wild leafy vegetables of the eastern cape province, South Africa. *Journal of Medicinal Plants Research*. 5(13): 2624-2628.

Jima, Megersa, 2018 – Jima, T.T., Megersa, M. (2018). Ethnobotanical Study of Medicinal Plants Used to Treat Human Diseases in Berbere District, Bale Zone of Oromia Regional State, South East Ethiopia. *Evidence-Based Complementary and Alternative Medicine*. DOI: <https://doi.org/10.1155/2018/8602945>

Momodu et al., 2014 – Momodu, O., Enogieru, A., Omoruyi, S., Om`Iniabo, F.A.E. (2014). Extracts of *Hunteria umbellata* reverses the effect of streptozotocin-induced pancreatic islet-cell destruction. *Journal of Experimental and Clinical Anatomy*. 13(2): 66. DOI: <https://doi.org/10.4103/1596-2393.154404>

Nazar et al., 2016 – Nazar, C.M.J., Bojerenu, M.M., Safdar, M., Ahmed, A., Akhtar, M.H., Kindratt, T.B. (2016). Efficacy of dietary interventions in end-stage renal disease patients; a systematic review. *Journal of Nephro pharmacology*. [Electronic resource]. URL: <http://www.ncbi.nlm.nih.gov/pubmed/28197497> <http://www.pubmedcentral.nih.gov/articlerender.fcgi?artid=PMC5297504>

Oboh et al., 2019 – Oboh, G., Adebayo, A.A., Ademosun, A.O., Abegunde, O.A. (2019). Aphrodisiac effect of *Hunteria umbellata* seed extract: Modulation of nitric oxide level and arginase activity in vivo. *Pathophysiology*. 26(1): 39-47. DOI: <https://doi.org/10.1016/j.pathophys.2018.11.003>

Oluwamodupe Cecilia Ejelonu, 2019 – Oluwamodupe Cecilia Ejelonu (2019). Mechanisms of action of aqueous extract from the *Hunteria umbellata* seed and metformin in diabetes. *World Journal of Meta Analysis*. 7(9): 418-422.

Pereira et al., 2019 – Pereira, A.S.P., Banegas-Luna, A.J., Peña-García, J., Pérez-Sánchez, H., Apostolides, Z. (2019). Evaluation of the anti-diabetic activity of some common herbs and spices: Providing new insights with inverse virtual screening. *Molecules*. 24(22). DOI: <https://doi.org/10.3390/molecules24224030>

Rec. GSCC (DGKC), 1972 – Rec. GSCC (DGKC) (1972). Optimized standard colorimetric methods. *Journal of Clinical Chemistry and Clinical Biochemistry*. 10: 182.

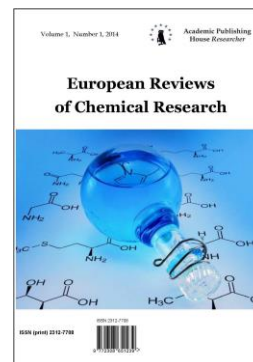
Reitman, Frankel, 1957 – Reitman, S., Frankel, S. (1957). A colorimetric method for the determination of serum glutamic oxaloacetate and glutamic pyruvic transaminase. *Amer. J. clinical pathology*. 28: 56-63.

Copyright © 2020 by Academic Publishing House Researcher s.r.o.



Published in the Slovak Republic
European Reviews of Chemical Research
Has been issued since 2014.
E-ISSN: 2413-7243
2020, 7(1): 20-36

DOI: 10.13187/erch.2020.1.20
www.ejournal14.com



Solvatochromic and Halochromic Evaluation of Some Biheterocyclic Cyanine Dyes

H.A. Shindy ^{a,*}, M.A. El-Maghraby ^a, F.M. Eissa ^a

^a Department of Chemistry, Faculty of Science, Aswan University, Aswan 81528, Egypt

Abstract

In the present study, the electronic absorption spectra of some biheterocyclic cyanine dyes having furan and pyrazole nucleus was recorded and investigated in a number of 6 (six) pure solvents having different polarities [water (78.54), D.M.F (36.70), ethanol (24.3), chloroform (4.806), CCl_4 (2.238) and dioxane (2.209)], mixed solvents [DMF- H_2O] and/or in a series of 8 (eight) aqueous universal buffer solutions having varied pH values [1.65, 2.32, 4.62, 5.85, 6.41, 7.82, 9.61 and 11.63 units] to evaluate their solvatochromic and/or halochromic properties, respectively. The dyes were thought to be better solvatochromic dyes when they give strong positive and/or negative solvatochromism in pure solvents having different polarities. Consequently, the solvatochromic of the dyes decrease when they give weak positive and/or negative solvatochromism in pure solvents having different polarities. In addition, the dyes were thought to be better halochromic dyes when they give strong positive and/or negative halochromism in aqueous universal buffer solutions having varied pH values. Consequently, the halochromic of the dyes decrease when they give weak positive and/or negative halochromism in aqueous universal buffer solutions having varied pH values. The study covers two different types of cyanine dyes. It includes, bis dimethine cyanine dyes and di-tri mixed methine cyanine dyes.

Keywords: cyanine dyes, solvatochromic dyes, halochromic dyes, acid-base properties, solvent effects, absorption spectra.

1. Introduction

Cyanine dyes (Shindy, 2012; Shindy, 2016; Shindy, 2017; Shindy, 2018; Shindy, 2019; Shindy, 2020) are important class of functional dyes and possesses an excellent, unique, superior and exceptional photochemical and photophysical properties, such as high molar extinction coefficients (molar absorptivity), tunable fluorescence intensities, narrow absorption bands, moderate quantum yields and absorb light mainly in the visible region, but also include and/or cover UV and NIR regions, larger than any other class of dye system. Therefore, an extensive number of cyanine dyes have been synthesized and developed for numerous applications in photographic processes and more recently as fluorescent probes for bio-molecular labeling and imaging (Mishra, et al., 2000; Pisoni, et al., 2014; Wada, et al., 2015; Hyun, et al., 2014; Hyun, et al., 2015; Njiojob, et al., 2015; Hyun, et al., 2015a; El-Shishtawy, et al., 2010; Henary and Levitz, 2013). On the other side, pyrazole compounds (Perrin, 1972; Eicher and Hauptmann, 2003; Panda and Jena, 2012; Hu, et al., 2012) are reported to possess a wide range of biological activities in literature such as anti-microbial, anti-fungal, anti-tubercular, anti-inflammatory, anti-convulsant,

* Corresponding author

E-mail addresses: hashindy2@hotmail.com (H.A. Shindy)

anti-cancer, anti-viral, angiotensin converting enzyme (ACE) inhibitory, neuroprotective, cholecystokinin-1 receptor antagonist, and estrogen receptor (ER) ligand activity and others (Katz, et al., 1965; Lango, Valentina, 2007). In addition, furan based substituted compounds (Chandrashekarachar, Kesagudu, 2017) showed very promising biomaterials such as anti-microbial, anti-cancer, anti-hyperglucemic and analgesic. Furan poly substituted compounds are employed as building blocks of synthesis of naturally occurring biomaterials which are important in medicinal chemistry. Besides, solvatochromic (Panigrahi, et al., 2013; Berezin, et al., 2007; Zimmermann, Machado, 2009) compounds attracted much attentions in the application of fluorescent probe, indicator, chromogenic reagent and molecular recognition field. Spectroscopic changes observed when solvatochromic dyes are dissolved in various media have been used to evaluate the polarity, temperature and the viscosity of the microenvironment in solution. Such dyes are useful as optical probes when a small perturbation causes large changes in the spectroscopic properties. Furthermore, halochromic (Zimmermann, Machado, 2009; Mazieres et al., 2009; Bussemer et al., 2009; Puyol et al., 2006) materials are used in chemical indicators, such as universal indicator, which indicates over a pH range of 1-14 with a continuous colour scale. These materials detect alterations in the acidity of substances, like detection of corrosion in metals. They are also suited for use in environments where pH changes occur frequently, or places where changes in pH are extreme.

Based on the former concepts we studied here the solvatochromism and halochromism (acid-base properties) of some biheterocyclic cyanine dyes containing furan and pyrazole nucleus, with the hope that a combination of the favourable properties of both furan, pyrazole and cyanine dyes may be achieved. In addition, this study shed the light on the best practical conditions when these dyes are used and/or applied as photosensitizers. Besides, this study is performed to evaluate the solvatochromic and halochromic properties of the investigated cyanine dyes to may be used and/or applied as solvatochromic and/or halochromic materials in any of the diverse and a broad area of many heterogenous fields, such as chemistry, biology and medicine.

Experimental

The investigated cyanine dyes were prepared in a way that described before (Shindy et al., 2002; Shindy et al., 2006). The molecular structures of the examined cyanine dyes [bis dimethine cyanine dye (1) and di-tri mixed methine cyanine dye (2)] are shown in Scheme 1 (Shindy et al., 2002; Shindy et al., 2006).

The organic solvents were of spectroscopic grade or were purified according to recommended methods (Shindy et al., 2014; Shindy et al., 2014a).

The electronic absorption spectra of the dyes were recorded on UV-VIS recording spectrophotometer using 1 cm cells Quartz. The stock solutions were about 1×10^{-3} M. Lower molarities were obtained by accurate dilution. The spectra were recorded immediately in order to eliminate as much as possible the effect of time.

For mixed solvents studying, an accurate volume of the stock solution (1×10^{-3} M in ethanol) of the dye was placed in 10 ml measuring flask containing the required volume of ethanol, then completed to the mark with the other solvent.

For aqueous universal buffer studying, an accurate volume of the stock solution was added to 5 ml of the buffer solution in a 10 ml volumetric flask, then diluted to the mark with redistilled water. The pH was checked before spectral measurements.

The aqueous universal buffer solution is prepared as a modified buffer series derived from that of Britton (Shindy et al., 2014; Shindy et al., 2014a). The constituents are as follows:

a. 0.4 M solution of phosphoric acid and 0.4 M acetic acid was prepared by dilution of the concentrated stock.

b. A solution of 0.4 M boric acid was obtained by dissolving the recrystallized acid in redistilled water.

c. A stock acid mixture was prepared by mixing equal volumes of the three acids. The total molarity of the acid was thus maintained at 0.4 M.

A series of buffer solutions with varied pH values ranging from (1.65-11.63) was prepared by mixing 150 ml of the acid mixture in a 250 ml volumetric flask with an appropriate volume of 1.0 M NaOH and diluted to the mark with redistilled water. The pH's of the buffer solutions were checked using an Orion pH-meter model (60iA) accurate to 0.005 pH units at 25 °C.

3. Results and discussion

3.1. Solvatochromic evaluation

Solvatochromic properties evaluation for the bis dimethine cyanine dye (1) and di-tri mixed methine cyanine dye (2) was carried out via examining of their electronic visible absorption spectra in pure solvents having different polarities. The dyes were thought to be better solvatochromic dyes when they give strong positive and/or negative solvatochromism in pure solvents having different polarities. Consequently, the solvatochromic of the dyes decrease when they give weak positive and/or negative solvatochromism in pure solvents having different polarities. So, we may say that the solvatochromic of one dye is higher than the other one if the positive and/or the negative solvatochromism in pure solvents having different polarities of the former one is stronger than that of the later one. In contrary, we may say that the solvatochromic of one dye is lower than the other one if the positive and/or the negative solvatochromism in pure solvents having different polarities of the former one is weaker than that of the latter one. (Shindy, 2019; Shindy et al., 2020). Positive solvatochromism reveals bathochromic shifted (red shifted) absorption bands with increasing solvent polarity. In contrast, negative solvatochromism discloses hypsochromic shifted (blue shifted) bands with increasing solvent polarity. This study was carried out to select the best solvents to use of these dyes as photosensitizers when there are applied in photosensitive material industry. The other important purpose of this study is to evaluate the solvatochromic properties of these dyes to may be used and/or applied as probes for determining solvent polarity, in physical, physical organic, inorganic and/or in solution chemistry.

The electronic absorption spectra of the bis dimethine cyanine dye (1), di-tri mixed methine cyanine dye (2) in pure solvents of different dielectric constant viz. water (78.54), D.M.F (36.70), ethanol (24.3), chloroform (4.806), CCl_4 (2.238) and dioxane (2.209) (Shindy et al., 2014; Shindy et al., 2014a) are recorded, Figure 1. The λ_{max} and ϵ_{max} values of the absorption bands due to different electronic transitions within the solute molecule in these solvents are represented in Table 1.

From Table 1, it's clearly that the electronic absorption spectra of the dyes in ethanolic medium are characterized by the presence of one essential absorption bands. These bands can be assigned to intramolecular charge transfer transitions (Shindy et al., 2014; Shindy et al., 2014a). These charge transfer is essentially due to transfer of lone pair of electrons from both pyrazole nitrogen atom and furan oxygen atom to the two positively charged quaternary quinolinium salt residue, Scheme 2.

The data given in Table 1 show that the charge transfer band exhibits a hypsochromic shift in ethanol relative to DMF, dioxane, $CHCl_3$ and CCl_4 . This effect may be attributed to the following factors:

a. The bathochromic shift in DMF relative to ethanol is a result of the increase in solvent polarity due to the increasing of dielectric constant of DMF relative to ethanol.

b. The hypsochromic shift occur in ethanol relative to dioxane, $CHCl_3$ and CCl_4 is result of the solute-solvent interaction through intermolecular hydrogen bond formation between ethanol and the lone pair electrons of both the pyrazole nitrogen atom and the furan oxygen atom, Scheme 3. This decreases slightly the electron density on the pyrazole nitrogen atom and furan oxygen atom and consequently decreases to some extent the mobility of the attached π -electrons over the conjugated pathway system to the positively charged heterocyclic quaternary salt residue, and accordingly blue shifts are occurs.

The unexpected hypsochromic shift in the λ_{max} of the longer wavelength charge transfer in water relative to ethanol and the other solvents, as well as it's lower extinction coefficients can be mainly ascribed to the possible interaction of water molecules with the lone pair electrons of pyrazole nitrogen atom and furan oxygen atom through hydrogen bond formation, Scheme 4. This makes difficult the transfer of charge to the quaternary heterocyclic residue and consequently there is observed a hypsochromic shift in water relative to ethanol and the other solvents, Table 1.

3.2. Solvatochromism in mixed solvents

This study is performed to trace the possibility of the formation of a hydrogen bonded solvated complex between the solute and solvent molecules. The complexes which are liable to form in solution are those of compounds capable of forming stable hydrogen bond between solute and solvent.

The electronic absorption spectra of 1.00×10^{-4} M of the bis dimethine cyanine dye (1) and di-tri mixed methine cyanine dye (2) in DMF containing varying amounts of H_2O is shown in

Figure 2. It's shown in the presence of 11.1 M of H₂O the spectrum exhibits bands at 524 nm for (1) and 529 nm for (2), respectively. While in the presence of 22.2 M, 33.3 M, 44.4 M, 55.6 M the bands is blue shifted to 515, 511, 503 and 501 nm for (1); 519, 516, 507 and 505 nm for (2), respectively. Also, a decrease in band intensity at fixed wavelength [550 nm (1); 530 nm (2)] is observed on increasing of H₂O concentration, See [Figures \(3, 4\)A, A](#).

The decreases in absorbance as well as the gradual blue shift in the maximum absorption wavelength on increasing the H₂O content can be ascribed to the gradual formation of the complex species through intermolecular hydrogen-bonding.

The graphical representation of absorbance at 550 nm for (1); 530 nm for (2) against the mole fraction of H₂O results that the absorbance decreases gradually with increasing the mole fraction of H₂O. See [Figures \(3, 4\)B, B](#).

To investigate the effect of the dielectric constant of the medium on the band shift (γ), on plotting versus $D-1/D+1$ ([El-Ezaby et al., 1970](#); [Gangaly, Banerjee, 1978](#)), broken line was obtained. See [Figures \(3, 4\)D](#).

Furthermore another broken line was obtained on plotting the absorbance against the dielectric constant of the medium. See [Figures \(3, 4\)C](#). Such behavior indicates that factors other than the change in the dielectric constant of the medium are responsible for the shift of λ_{\max} at lower and higher percentage of H₂O. These factors mainly include the solute solvent interaction through intermolecular hydrogen bonding which leads to the formation of some molecular complexes.

On plotting the excitation energy (E) versus the mole fraction of H₂O, See [Figures \(3, 4\)E](#), a broken line with three segments was obtained. The first segment represents the orientation of the solvent molecules around the solute. The second segment corresponds to the molecular complex formation, where is the third one represents the steady state of energy attained after complete of the molecular complex. From the above relation, it is clear that the position of the band and consequently the excitation energy depends not only on the mole fraction of H₂O, but also on the followings:

- a. Solvation energy.
- b. Orientation of the solvent molecule around the solute molecule in the ground and excited states.
- c. Dipole moment of the solute in both ground and excited states.
- d. Dipole-Dipole interaction between the solute and the solvent.
- e. The strength of the hydrogen bonding between the solute and the solvent in both the ground and the excited states.

In pure DMF solution, the dye molecule forms a solvent cage, which is affected on adding H₂O. At lower H₂O content, H₂O molecules will distribute themselves uniformly on all the solvation sheathes around the molecule. The added molecules may first enter the outer solvation sheathes and then will introduce themselves in the first sheathes as their proportions are increased. This probably due to the fact that addition of H₂O permit the formation of the solvent cage around the solute molecules, through intermolecular hydrogen bonding which is previously discussed.

From [Figures \(3, 4\)E](#) and [Table 2](#) it is possible to evaluate the excitation energy of the solute in the pure H₂O as equal to 57.1 Kcal/mol (comp. 1); 56.6 Kcal/mol (comp. 2), whereas the value in pure DMF amounts to 54.3 K cal/mol (comp. 1); 53.7 K cal/mol (comp. 2). The difference between the excitation energy in pure DMF and that corresponding to the first inflection point amounts to 0.30 Kcal/mol (comp. 1); 0.4 Kcal/mol (comp. 2). This value corresponds to the orientation energy of the solvent molecules around the solute molecules ([El-Ezaby et al., 1970](#); [Gangaly, Banerjee, 1978](#)). See [Figures \(3, 4\)E, Table 2](#).

The plot of E and ΔE against the mole fraction of H₂O results broken lines (see [Figures \(3, 4\)E; \(3, 4\)F, Table 2](#)) indicating that the excitation energy depends on factors other than the mole fraction of H₂O. From the above relation it was observed that the orientation energy is equal to 0.90 Kcal/mol (comp. 1), 1.00 Kcal/mol (comp. 2) and the hydrogen bond energy equal to 0.50 Kcal/mol (comp. 1), 0.30 Kcal/mol (comp. 2), see [Table 2](#).

3.3. Halochromic evaluation

Halochromic properties evaluation for the bis dimethine cyanine dye (1) and di-tri mixed methine cyanine dye (2) was carried out by investigated of their electronic visible absorption

spectra in aqueous universal buffer solutions having varied pH values, [Figure 5](#). The dyes were thought to be better halochromic dyes when they give strong positive and/or negative halochromism in aqueous universal buffer solutions having varied pH values. Consequently, the halochromic of the dyes decrease when they give weak positive and/or negative halochromism in aqueous universal buffer solutions having varied pH values. So, we may say that the halochromic of one dye is higher than the other one if the positive and/or the negative halochromism of the former one in aqueous universal buffer solutions having varied pH values is stronger than that of the latter one. In contrary, we may say that the halochromic of one dye is lower than the other one if the positive and/or the negative halochromism of the former one in aqueous universal buffer solutions having varied pH values is weaker than that of the latter one. ([Shindy, 2019](#); [Shindy et al., 2020](#)). Positive halochromism means occurrence of a bathochromic shifted (red shifted) absorption bands with changing solution pH of the buffer solution. In contrast, negative halochromism means occurrence of a hypsochromic shifted (blue shifted) absorption bands with changing the pH of the buffer solution.

The solutions of the bis dimethine cyanine dye (1) and di-tri mixed methine cyanine dye (2) have a permanent cationic charge in basic media which then discharged on acidification. This prompted our attention and encouraged us to study their spectral behavior in different buffer solutions in order to select a suitable pH for use of these dyes as photosensitizers. The other important purpose of this study is to evaluate the halochromic properties of these dyes to may be used and/or applied as indicators in operations of acid/base titrations in analytical chemistry. The acid dissociation or protonation constants of these dyes have been determined. The effect of the compounds as photosensitizers increase when they are present in the ionic form, which has a higher planarity ([Shindy et al., 2014](#); [Shindy et al., 2014a](#)), and therefore more conjugation.

The electronic spectra of the bis dimethine cyanine dye (1) and di-tri mixed methane cyanine dye (2) in aqueous universal buffer of varying pH values (ranging from 1.65 to 11.63 units) showed bathochromic shifts with intensification of their absorption bands at high pH (alkaline media) and hypsochromic shifts with quenching the intensity of the absorption bands at low pH (acidic media), [Figure 5](#).

So, the mentioned dyes which have free lone pairs of electrons on the pyrazole nitrogen atom and furan oxygen atom undergo protonation in low pH (acidic media). This leads to a criterion of positive charge on pyrazole nitrogen atom and furan oxygen atom and consequently the electronic charge transfer pathway to the quaternary heterocyclic quinolinium salt residue will be difficult resulting a hypsochromic shifts for the absorption bands.

On increasing the pH of the media, the absorption bands are intensified and bathochromically shifted due to deprotonation of the pyrazole nitrogen atom and furan oxygen atom and consequently the electronic charge transfer pathways to the quaternary heterocyclic quinolinium salt residue will be easier and facilitated resulting a bathochromic shifts for the absorption bands.

The charge transfer of the dyes is attributed to electronic transitions from both pyrazole nitrogen and furan oxygen atoms to the positively charged quinolinium 2-yl salt moiety, [Scheme 2](#). This electronic transitions are responsible for intensification of the absorption bands and the mesomeric interactions with the rest of the molecule, consequently the charge transfer band interaction within the free base is facilitated, [Scheme 2](#).

Several methods have developed for spectrophotometric determination of the dissociation constants of weak acids. The variation of absorbance with pH can be utilized ([Shindy et al., 2014](#); [Shindy et al., 2014a](#)). On plotting the absorbance at the λ_{\max} vs. pH, an S-shaped curves are obtained, [Figure 6](#), [Table 3](#).

An all of the S-shaped curves obtained, the horizontal portion to the left corresponds to the acidic form of the indicator, while the upper portion to the right corresponds to the basic form, since the pka is defined as the pH value for which one half of the indicator is in the basic form and the other half in the acidic form. This point is determined by intersection of the curve with a horizontal line midway between the left and right segments ([Shindy et al., 2014](#); [Shindy et al., 2014a](#)). The acid dissociation or protonation constants values of the dyes are summarized in [Table 3](#).

3. Conclusion

Following are major conclusions were drawn from the results discussed in this study:

1. The solvatochromism of the bis dimethine cyanine dye (1) and di-tri mixed methine cyanine dye (2) in pure solvents having different polarities underwent displacements to give positive solvatochromism (occurrence of a bathochromic shift with increasing solvent polarity) and/or negative solvatochromism (occurrence of a hypsochromic shift with increasing solvent polarity) depending upon the following factors:

a. Increasing and/or decreasing the polarity (the dielectric constant) of the solvent (general solvent effect).

b. Hydrogen bond and/or molecular complex formation between the solute (dyes molecules) and the solvent used (specific solvent effect).

2. The halochromism of the bis dimethine cyanine dye (1), di-tri mixed methine cyanine dye (2) in aqueous universal buffer solutions having varied pH values underwent displacements to give hypsochromic shifted and lower intensity bands in the lower pH media (acidic media). This is can be related to the protonated structures of the dyes in this media. In contrast, the bands of these dyes are intensified and bathochromically shifted in high pH media (basic media). This can be attributed to the deprotonated structures of the dyes in this media.

3. Solvatochromic evaluation of cyanine dyes can be determining through investigating their electronic absorption spectra in pure solvents having different polarities.

4. Halochromic evaluation of cyanine dyes can be made via examining their electronic absorption spectra in aqueous universal buffer solutions having varied pH values.

5. The trace of the possibility of the formation of a hydrogen bonded solvated complex between the solute (cyanine dyes) and solvent molecules can be performed by investigating the electronic absorption spectra of solute (cyanine dyes) in mixed solvents.

6. These cyanine dyes can be used as probes for determining solvent polarity in solution chemistry due to their solvatochromic properties.

7. These cyanine dyes can be used as acid-base indicators in analytical chemistry due to their halochromic properties.

8. Because cyanine dyes have multi purposes uses and applications in various fields and different research area, this research paper is recommended not only for heterocyclic and/or cyanine dyes chemists but also for other scientists in many and many heterogenous fields like biology, biotechnology, biochemistry, physics, engineering, pharmacology, medicine as well as environment and clinical analysis.

9. Furthermore, this study is recommended for all whom interested in the light absorbing systems in their research, labeling of biomolecules and/or in the synthesis and characterization of complex organic compounds

4. Conflict of interest

There is no conflict of interest.

5. Acknowledgements

We are thankful to the Chemistry department, Faculty of Science, Aswan University, Aswan, Egypt for supporting this work.

References

Berezin et al., 2007 – Berezin, M.Y., Lee, H., Akers, W., Achilefu, S. (2007). Near infrared dyes as lifetime solvatochromic probes for micropolarity measurements of biological systems. *Biophysical Journal*. 93: 2892-2899.

Bussemer et al., 2009 – Bussemer, B., Dreiling, I., Grummt, U., Mohr, G.J. (2009). Spectroscopic and quantum chemical study of the Bronsted acid sites in zeolite L channels with acidochromic cyanine dyes. *Journal of Photochemistry and Photobiology A: Chemistry*. 204: 90-96.

Chandrashekarachar, Kesagudu, 2017 – Chandrashekarachar, D., Kesagudu, D. (2017). Importance of furan based compounds and their biomedical applications: An overview. *Indo American Journal of Pharmaceutical Research*. 7(1): 7541-7549.

- Eicher, Hauptmann, 2003 – Eicher, T., Hauptmann, S. (2003). 2nd ed. New York: Wiley-VCH. The Chemistry of Heterocycles: Structure, Reactions, Synthesis and Applications.
- El-Ezaby et al., 1970 – El-Ezaby, M.S. Salem, I.H., Zewail, A.H., Issa, R.M. (1970). Spectral studies of some hydroxy-derivatives of anthraquinones. *J. Chem. Soc.* 13: 1293-1296.
- El-Shishtawy et al., 2010 – El-Shishtawy, R.M., Asiri, A.M., Basaif, S.A., Rashad Sobahi, T. (2010). Synthesis of a new beta-naphthothiazole monomethine cyanine dye for the detection of DNA in aqueous solution. *Spectrochim. Acta A.* 75: 1605-1609.
- Ganguly, Banerjee, 1978 – Ganguly, T., Banerjee, S.B. (1978). Effect of hydrogen bonding on the electronic absorption spectra of xylenols. *Spectrochim. Acta.* 34A: 617-623.
- Henary, Levitz, 2013 – Henary, M., Levitz, A. (2013). Synthesis and applications of unsymmetrical carbocyanine dyes. *Dyes Pigment.* 99: 1107-1116.
- Hu et al., 2012 – Hu J., Chen S., Sun Y., Yang J., Rao Y. (2012). Synthesis of tri- and tetrasubstituted pyrazoles via Ru(II) catalysis: Intramolecular aerobic oxidative C-N coupling. *Org Lett.* 14: 5030-5033.
- Hyun et al., 2014 – Hyun, H., Wada, H., Bao, K., Gravier, J., Yadav, Y., Laramie, M., Henary, M., Frangioni, J.V., Choi, H.S. (2014). Phosphonated Near-Infrared Fluorophores for Biomedical Imaging of Bone. *Angew. Chem. Int. Ed. Engl.* 53: 10668-10672.
- Hyun et al., 2015 – Hyun, H., Owens, E.A., Wada, H., Levitz, A., Park, G., Park, M.H., Frangioni, J.V., Henary, M., Choi, H.S. (2015). Cartilage-Specific Near-Infrared Fluorophores for Biomedical Imaging. *Angew. Chem. Int. Ed. Engl.* 54: 8648-8652.
- Hyun et al., 2015a – Hyun, H., Park, M.H., Owens, E.A., Wada, H., Henary, M., Handgraaf, H.J.M., Vahrmeijer, A.L., Frangioni, J.V., Choi, H.S. (2015). Structure-inherent targeting of near-infrared fluorophores for parathyroid and thyroid gland imaging. *Nat. Med.* 21: 192-197.
- Katz et al., 1965 – Katz, A.M., Pearson, C.M., Kennedy, J.M. (1965). A clinical trial of indomethacin in rheumatoid arthritis. *Clin Pharmacol Ther.* 6: 25-30.
- Lango, Valentina, 2007 – Lango, K., Valentina, P. (2007). 1st ed. India: Keerthi Publishers. Textbook of Medicinal Chemistry: 327-333.
- Mazieres et al., 2009 – Mazieres, M.R., Duprat, C., Wolf, J.G., Roshal, A.D. (2009). pH dependent spectral properties and electronic structure of benzothiazole containing cyanine dyes. *Dyes and Pigments.* 80: 355-360.
- Mishra et al., 2000 – Mishra, A., Behera, R.K., Behera, P.K., Mishra, B.K., Behera, G.B. (2000). Cyanines during the 1990s: A Review. *Chem. Rev.* 100: 1973-2012.
- Njiojob et al., 2015 – Njiojob, C.N., Owens, E.A., Narayana, L., Hyun, H., Choi, H.S., Henary, M. (2015). Tailored Near-Infrared Contrast Agents for Image Guided Surgery. *J. Med. Chem.* 58: 2845-2854.
- Panda, Jena, 2012 – Panda, N., Jena, A.K. (2012). Fe-catalyzed one-pot synthesis of 1,3-di- and 1,3,5-trisubstituted pyrazoles from hydrazones and vicinal diols. *J Org Chem.* 77: 9401-9406.
- Panigrahi et al., 2013 – Panigrahi, M., Patel, S., Mishra, B.K. (2013). Solvatochromism of some hemicyanine dyes. *Journal of Molecular Liquids.* 177: 335-342.
- Perrin, 1972 – Perrin, D.D. (1972). London: Butterworths. Dissociation Constants of Organic Bases in Aqueous Solution.
- Pisoni et al., 2014 – Pisoni, D.S., Todeschini, L., Borges, A.C.A., Petzhold, C. L., Rodembusch, F.S., Campo, L.F. (2014). Symmetrical and Asymmetrical Cyanine Dyes. Synthesis, Spectral Properties, and BSA Association Study. *J. Org. Chem.* 79: 5511-5520.
- Puyol et al., 2006 – Puyol, M., Encinas, C., Revera, L., Miltsov, S., Alonso, J. (2006). Synthesis of new ketocyanine dyes for the development of optical sensors, optical characterization and solvatochromic behavior. *Sensors and Actuators B.* 115: 287-296.
- Shindy et al., 2002 – Shindy, H.A., El-Maghraby, M.A., Eissa, F.M. (2002). Novel Cyanine Dyes: Synthesis, Characterization and Photosensitization-Structure Correlation. *Journal of the Chinese Chemical Society.* 49: 1061-1068.
- Shindy et al., 2006 – Shindy, H.A., El-Maghraby, M.A., Eissa, F.M. (2006). New Photosensitizers Cyanine Dyes: Synthesis and Properties. *Indian Journal of Chemistry.* 45B: 1197-1203.

[Shindy et al., 2014](#) – *Shindy, H.A., El-Maghraby, M.A., Eissa, F.M.* (2014). Synthesis and Spectral Properties of Novel Hemicyanine dyes. *Russ. Izv. AN. Ser. Khim.* 63(3): 707-715 [in Russian]

[Shindy et al., 2014a](#) – *Shindy, H.A., El-Maghraby, M.A., Eissa, F.M.* (2014). Effects of Chemical structure, solvent and solution pH on the visible spectra of some new methine cyanine dyes. *European Journal of Chemistry.* 5(3): 451-456.

[Shindy et al., 2020](#) – *Shindy, H.A., El-Maghraby, M.A., Goma, M.M., Harb, N.A.* (2020). Heptamethine and nonamethine cyanine dyes: novel synthetic strategy, electronic transitions, solvatochromic and halochromic evaluation. *Chemistry International*, 6 (4), 187-199.

[Shindy, 2012](#) – *Shindy, H.A.* (2012). Basics, Mechanisms and Properties in the Chemistry of Cyanine Dyes: A Review Paper. *Mini-Reviews in Organic Chemistry.* 9(4): 352-360.

[Shindy, 2016](#) – *Shindy, H.A.* (2016). Characterization, Mechanisms and Applications in the Chemistry of Cyanine Dyes: A Review. *European Journal of Molecular Biotechnology.* 14(4): 158-170.

[Shindy, 2017](#) – *Shindy, H.A.* (2017). Fundamentals in the Chemistry of Cyanine Dyes. *A Review Dyes and Pigments.* 145: 505-513

[Shindy, 2018](#) – *Shindy, H.A.* (2018). Structure and solvent effects on the electronic transitions of some novel furo/pyrazole cyanine dyes. *Dyes and Pigments.* 149: 783-788.

[Shindy, 2019](#) – *Shindy, H.A.* (2019). Different methods in the synthesis of polyheterocyclic cyanine dyes: A review. *European Journal of Molecular Biotechnology.* 7 (2): 109-122.

[Shindy, 2019](#) – *Shindy, H.A.* (2019). Synthesis of different classes of polyheterocyclic cyanine dyes: a Review. *European Reviews of Chemical Research*, 6 (1), 29-46.

[Shindy, 2020](#) – *Shindy, H.A.* (2020). Synthesis of different classes of five/six membered heterocyclic cyanine dyes: A review. *Chemistry International.* 6(2): 56-74.

[Wada et al., 2015](#) – *Wada, H., Hyun, H., Vargas, C., Gravier, J., Park, G., Gioux, S., Frangioni, J.V., Henary, M., Choi, H.S.* (2015). Pancreas-Targeted NIR Fluorophores for Dual-Channel Image-Guided Abdominal Surgery. *Theranostics.* 5: 1-11.

[Zimmermann, Machado, 2009](#) – *Zimmermann, L.M., Machado, V.G.* (2009). Chromogenic anionic chemosensors based on protonated merocyanine solvatochromic dyes: influence of the medium on the quantitative and naked-eye selective detection of anionic species. *Dyes and Pigments.* 82: 187-195.

Appendix

Table 1. Electronic Absorption Spectra of some biheterocyclic cyanine dyes (1) and (2) in pure solvents (Solvatochromism).

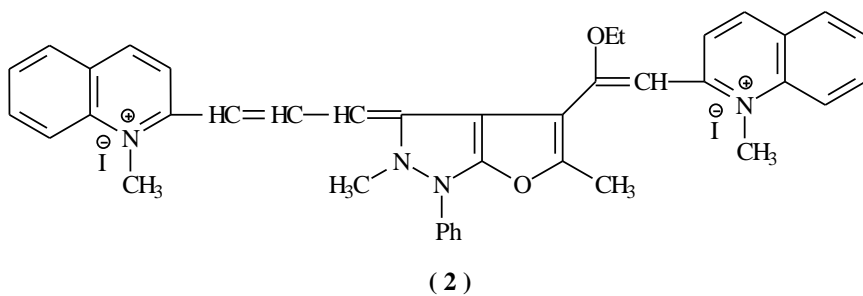
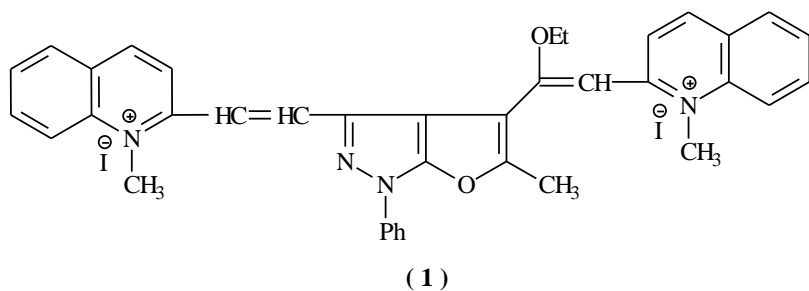
Comp. No.	Water		Ethanol		D.M.F		Chloroform		CCl ₄		Dioxane	
	λ_{\max} (nm)	ϵ_{\max} (cm ² mole ⁻¹)	λ_{\max} (nm)	ϵ_{\max} (cm ² mole ⁻¹)	λ_{\max} (nm)	ϵ_{\max} (cm ² mole ⁻¹)	λ_{\max} (nm)	ϵ_{\max} (cm ² mole ⁻¹)	λ_{\max} (nm)	ϵ_{\max} (cm ² mole ⁻¹)	λ_{\max} (nm)	ϵ_{\max} (cm ² mole ⁻¹)
1	496	16060	502	7890	513	19630	512	18560	503	11040	502	11580
	—	—	—	—	396	16460	514	14730	425	10770	420	10700
2	493	18170	508	14220	518	12630	513	15750	515	12930	513	18240
	—	—	—	—	396	7910	411	12860	519	14100	411	16140

Table 2. Commutative Data Obtained for some biheterocyclic cyanine dyes (1) and (2) in Mixed Solvents (D.M.F.-H₂O mixture)

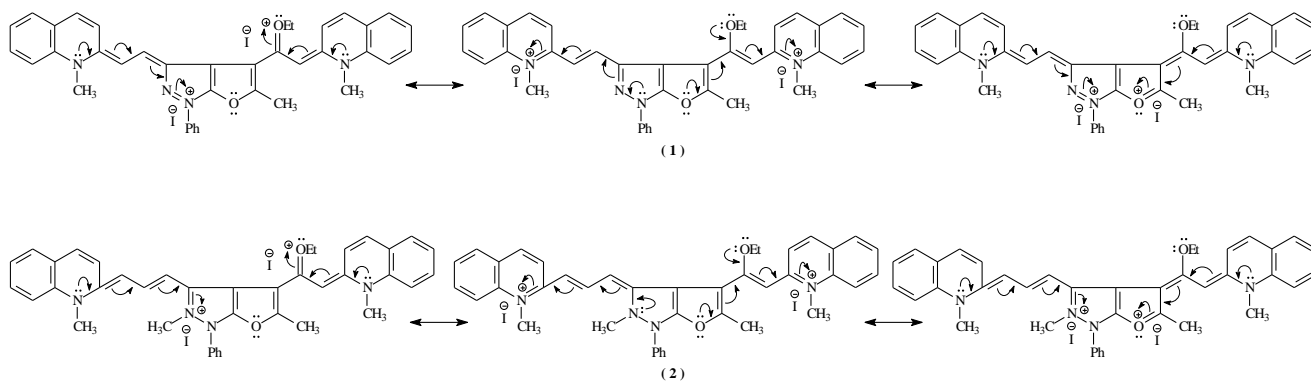
Comp. No.	Excitation Energy in Pure Solvents (kcal./mol.)		Excitation Orient Energy (kcal./mol.)	Excitation H-bond Energy (kcal./mol.)	Total Excitation Energy (kcal./mol.)
	D.M.F.	H ₂ O			
1	54.30	57.10	0.90	0.50	1.40
2	53.70	56.40	1.00	0.30	1.30

Table 3. The variation of absorbance with pH at fixed λ for some biheterocyclic cyanine dyes (1) and (2) in aqueous universal buffer solutions

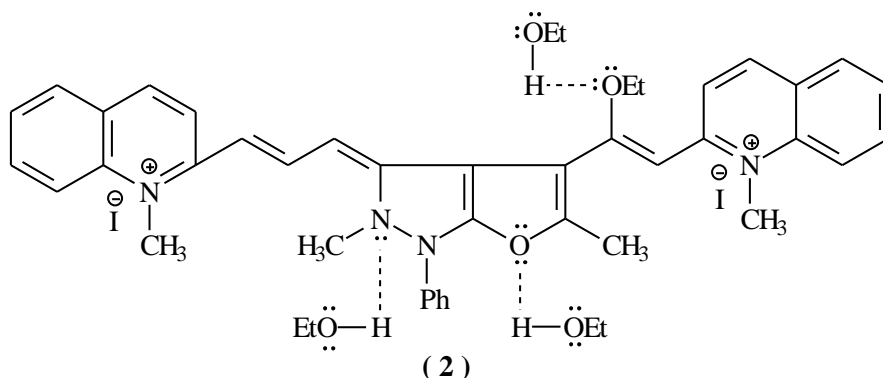
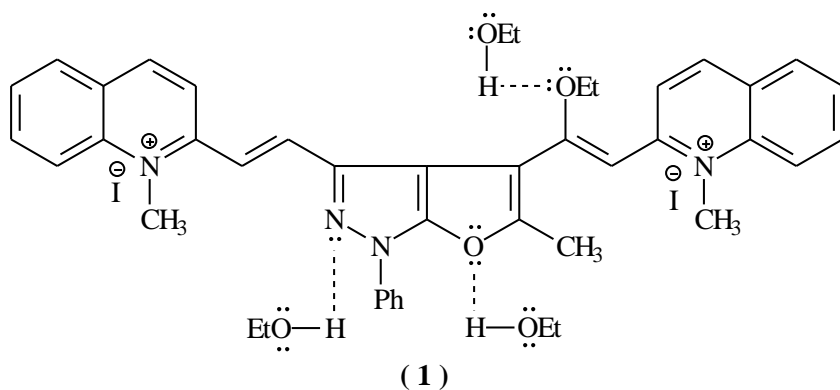
pH	Absorbance	
	(1)	(2)
	$\lambda = 510$ (nm)	$\lambda = 585$ (nm)
1.65	0.35	0.31
2.32	0.71	0.48
4.62	0.86	0.62
5.85	0.82	0.57
6.41	0.82	0.55
7.82	0.82	0.66
9.61	0.87	0.65
11.63	0.89	0.64
pKa	2; 9	2.6; 8.4



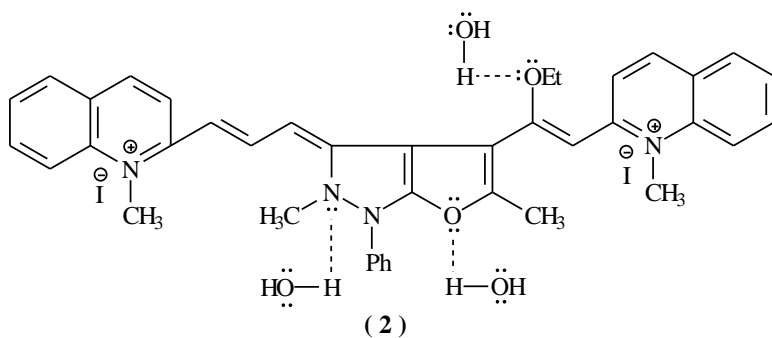
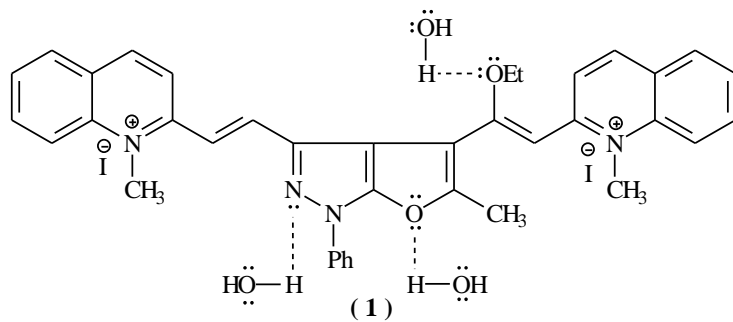
Scheme 1. Molecular structures of the bis dimethine cyanine dye (1) and di-tri mixed methine cyanine dye (2)



Scheme 2. Electronic transitions pathways illustration of the bis dimethine cyanine dye (1) and di-tri mixed methine cyanine dye (2)



Scheme 3. Hydrogen bond formation between the bis dimethine cyanine dye (1), di-tri mixed methine cyanine dye (2) and ethanol molecules (specific solvent effect)



Scheme 4. Hydrogen bond formation between the bis dimethine cyanine dye (1), di-tri mixed methine cyanine dye (2) and water molecules (specific solvent effect)

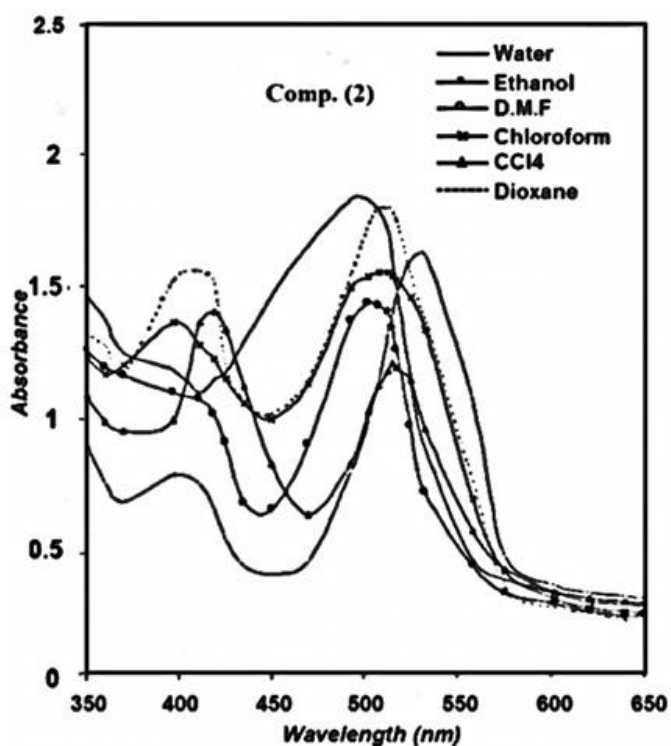
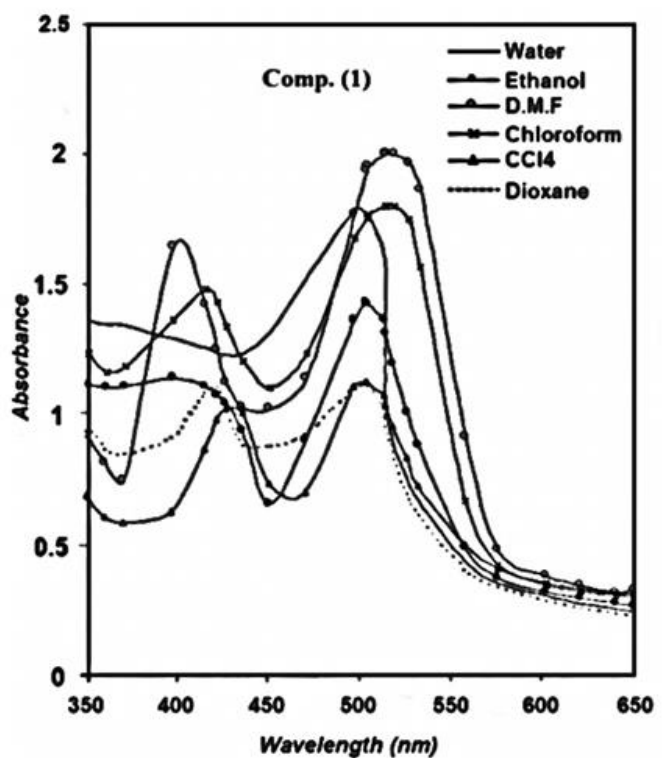


Fig. 1. Solvatochromism of the bis dimethine cyanine dye (1) and di-tri mixed methine cyanine dye (2) in pure solvents

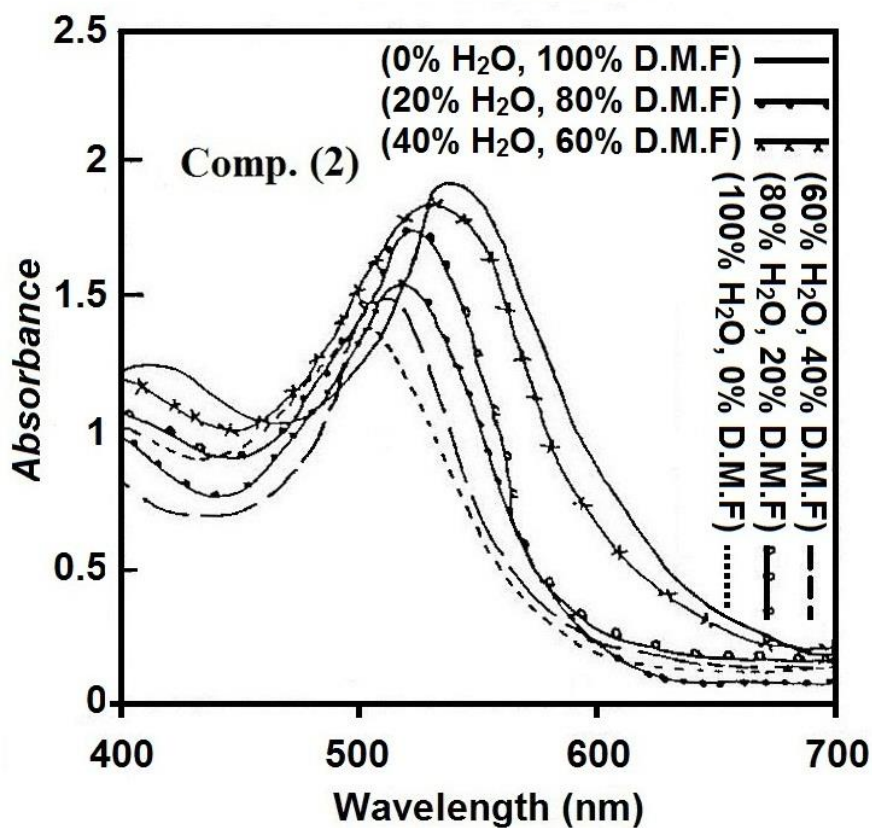
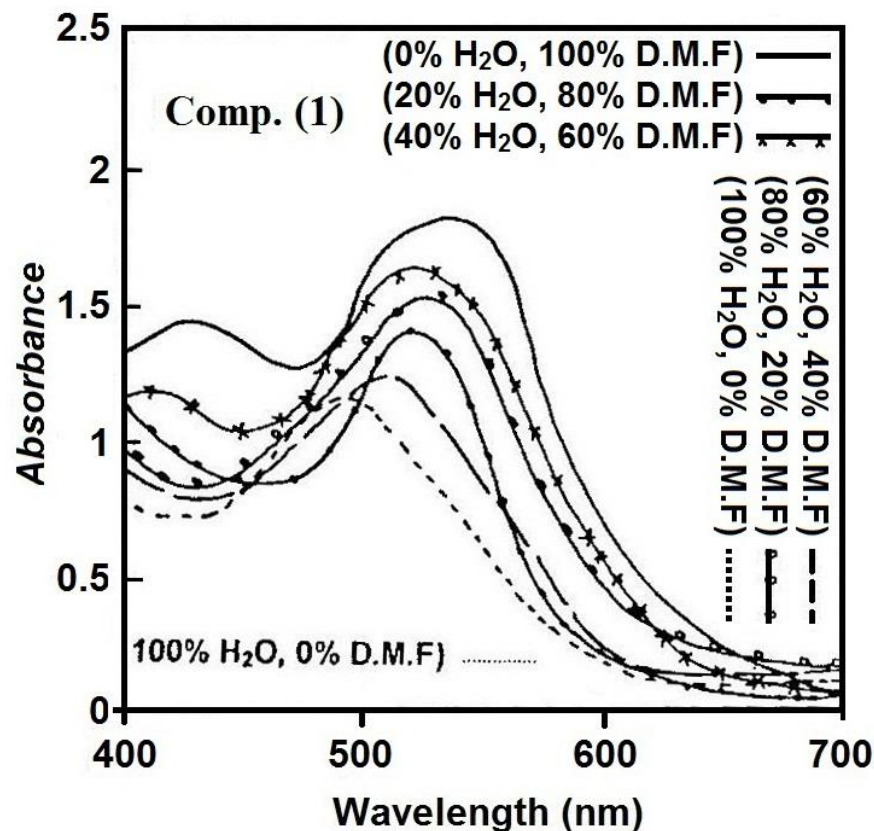


Fig. 2. Solvatochromism of the bis dimethine cyanine dye (1) and di-tri mixed methine cyanine dye (2) in mixed solvents

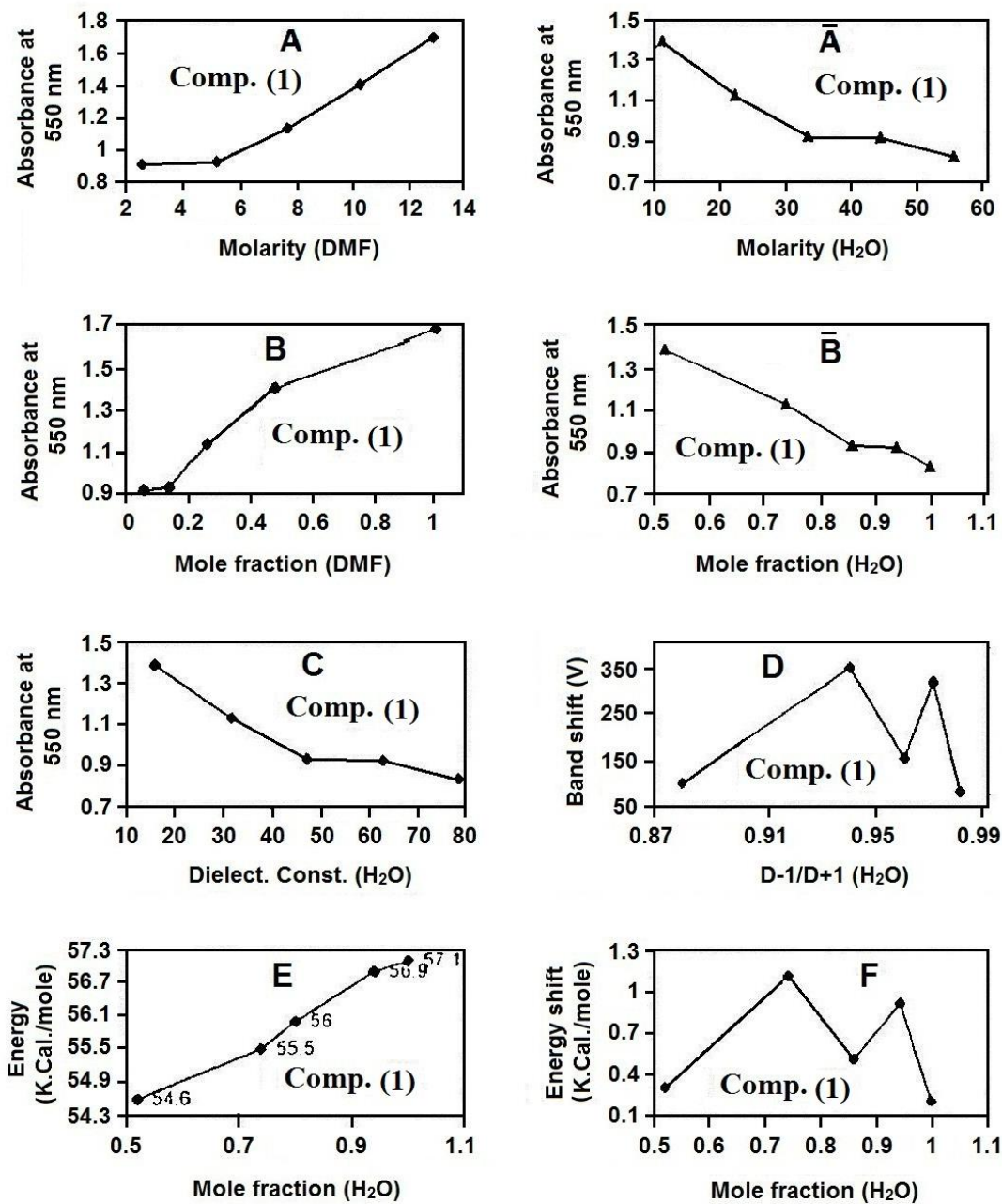


Fig. 3. Various illustration relation curves of the bis dimethine cyanine dye (1) in mixed solvents

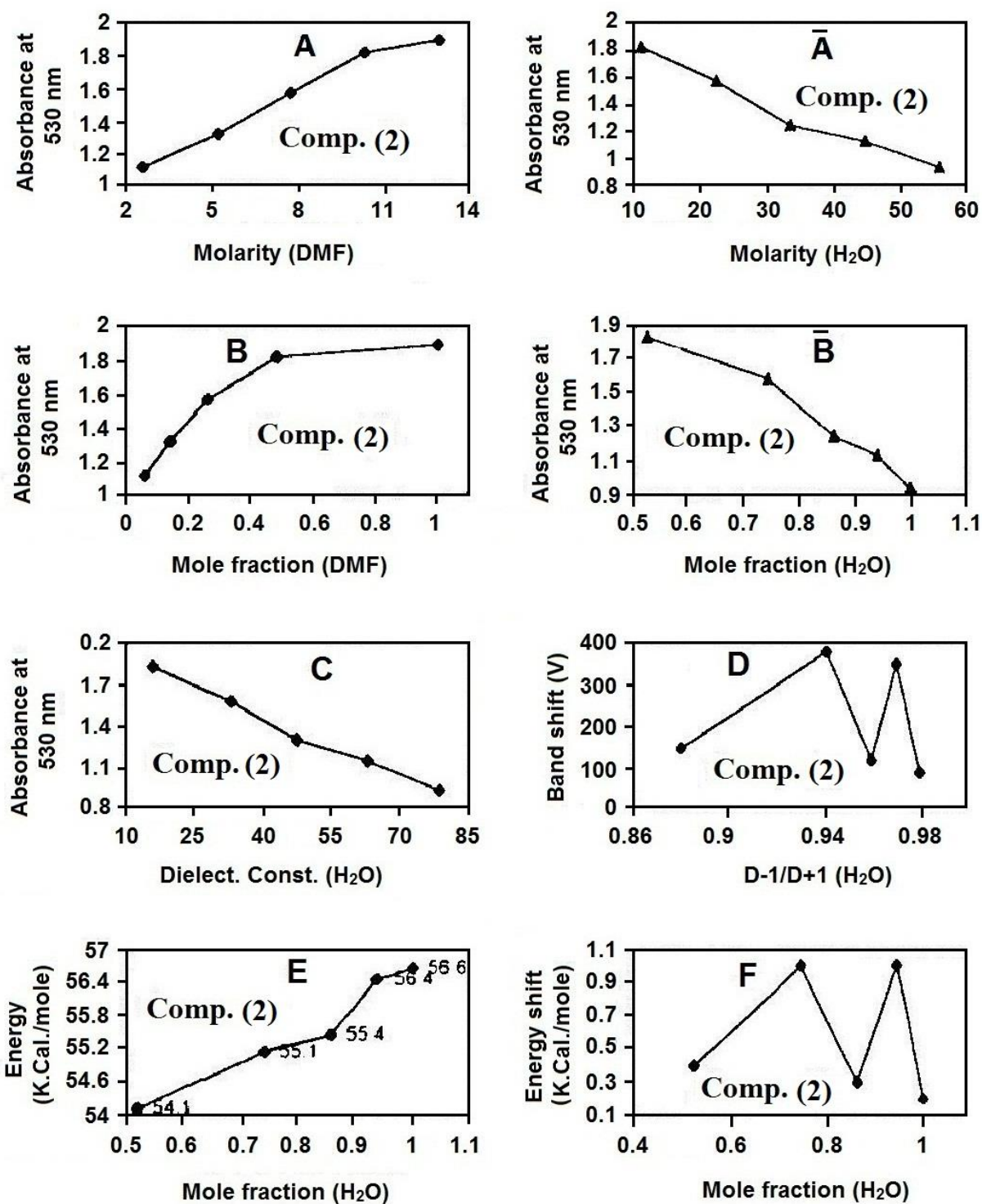


Fig. 4. Various illustration relation curves of the di-tri mixed methane cyanine dye (2) in mixed solvents

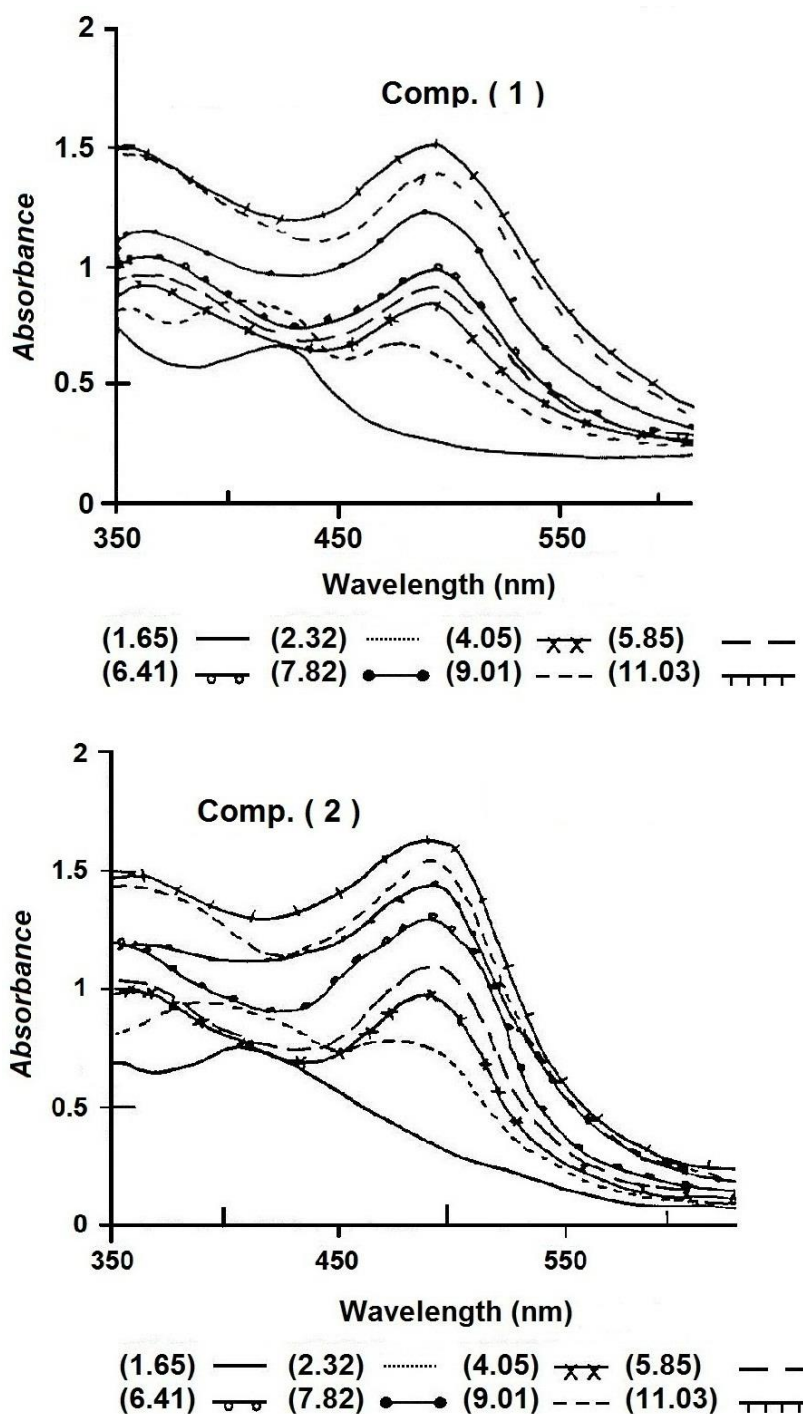


Fig. 5. Halochromism of the bis dimethine cyanine dye (1) and di-tri mixed methine cyanine dye (2) in aqueous universal buffer solutions

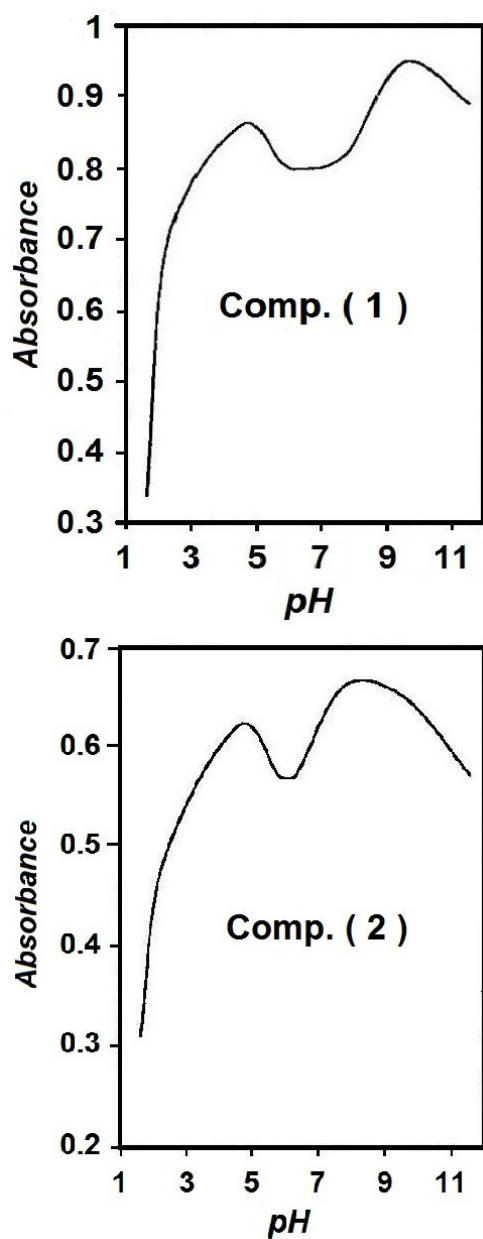


Fig. 6. Acid-base S-Curves of the bis dimethine cyanine dye (1) and di-tri mixed methine cyanine dye (2)